Bureau of Mines Report of Investigations/1983

Thermal and Electrical Ignitability of Dust Clouds

By Ronald S. Conti, Kenneth L. Cashdollar,
Martin Hertzberg, and Israel Liebman

UNITED STATES DEPARTMENT OF THE INTERIOR

Report of Investigations 8798

Thermal and Electrical Ignitability of Dust Clouds

By Ronald S. Conti, Kenneth L. Cashdollar,
Martin Hertzberg, and Israel Liebman

UNITED STATES DEPARTMENT OF THE INTERIOR
James G. Watt, Secretary

BUREAU OF MINES
Robert C. Horton, Director

Library of Congress Cataloging in Publication Data:

Thermal and electrical ignitability of dust clouds.

(Bureau of Mines report of investigations ; 8798)

Bibliography: p. 38-40.

Supt. of Docs. no.: I 28.23:8798.

1. Dust explosion. I. Conti, R. S. (Ronald S.). II. Series: Report of investigations (United States. Bureau of Mines) ; 8798.

TN23.U43 [QD516] 622s [622'.8] 83-600174

CONTENTS

ILLUSTRATIONS

ILLUSTRATIONS--Continued

TABLES

UNIT OF MEASURE ABBREVIATIONS USED IN THIS REPORT

atm	atmosphere	m	meter
°C	degree Celsius	mg	milligram
cal/g	calorie per gram	min	minute
cm	centimeter	mm	millimeter
cm^3	cubic centimeter	msec	millisecond
g	gram	µF	microfarad
g m^{-3}	gram per cubic meter	µm	micrometer
J	Joule	pct	percent
kV	kilovolt	sec	second
L	liter	V	volt
L/kg	liter per kilogram		

THERMAL AND ELECTRICAL IGNITABILITY OF DUST CLOUDS

By Ronald S. Conti,[1] Kenneth L. Cashdollar,[2] Martin Hertzberg,[3] and Israel Liebman[4]

ABSTRACT

The Bureau of Mines conducted a comprehensive laboratory study of the thermal ignitability of various carbonaceous dust clouds with particular emphasis on various ranks of coal dust. The tests were conducted using a new 1.2-L furnace. Autoignition temperatures of dust clouds were obtained as a function of coal volatility and particle size. Dust particles and gas samples were collected by a rapid-sampling system in order to study the reactions involved in preignition and postignition processes. The autoignition temperatures measured in the new 1.2-L furnace were significantly lower and therefore more conservative than those measured previously in the Godbert-Greenwald furnace.

The combined effects of thermal and electrical ignition of dust clouds were also studied in the 1.2-L furnace using electrical discharges of varying energies at ambient and elevated temperatures. The minimum spark energy necessary to ignite a dust cloud decreased significantly as the temperature of the dust cloud increased.

[1]Electronics engineer.
[2]Physicist.
[3]Supervisory research chemist.
[4]Supervisory research physicist (retired).
Pittsburgh Research Center, Bureau of Mines, Pittsburgh, Pa.

INTRODUCTION

Dust explosions constitute a persistent hazard to life and property in many industrial and commercial establishments. In mines and industrial plants, the safety problem is aggravated by the presence of flammable gas. Although the destructive effects of dust and gas explosions are comparable, the dust hazard is more insidious in some ways. Near the outcrops of coal seams or in shallow mines, gas emissions are small and infrequent. The same is true of occasional emissions from well designed and maintained industrial plants or gas appliances used in commercial establishments and in homes. Such occasional gas leakage is usually diluted, rendered harmless, and removed by normal ventilation flows. Dust, on the other hand, is not effectively removed by ventilation and inevitably accumulates within a system. Thus the probability of an explosion from its presence increases continuously during the operation of the system unless special precautions are taken to remove those accumulations or to neutralize their presence.

In the worst 1-year period in U.S. mining history, from December 1907 to December 1908, more than 1,000 coal miners were killed in explosions (19).[5] The public's reaction to those disasters led eventually to the establishment by Congress of the Bureau of Mines, with specific authority to inquire as to the causes of those disasters. Over the decades of this century, as research illuminated the causes, as preventive measures were introduced, and as safety regulations were promulgated and enforced, the fatality rate from such explosions declined steadily from decade to decade. In the 1970's the explosion fatality rate averaged seven deaths per year. Unfortunately, as a result of several disasters, the period from April 1981 to April 1982 was the worst since the passage of the Coal Mine Health and Safety Act of 1969, and the new decade of the 1980's began with 4 major explosion disasters involving 43 fatalities during that 1-year period (29).

Most of the coal produced in the United States is eventually pulverized into a dust and then pneumatically fed into the burners of boiler furnaces in order to produce steam for electric power generation. Explosions are a persistent hazard at all stages of the power generation process, from coal production at the mine face to coal combustion in the powerplant. Hazards are present not only from unintended dust accumulations in the work spaces of such facilities, but also in the internal workings of equipment that is used to transport, clean, crush, dry, pulverize, and burn the coal. Comparable dust explosion hazards are found in other industries: Agricultural dusts are involved in grain elevators, storage facilities, and food processing plants; metallic dusts are involved in industries that produce, fabricate, and machine metals or that specifically use metallic dusts. An enormous variety of hydrocarbonaceous dusts are produced, handled, and used by the primary chemical industries in plastics, pharmaceuticals, dyes, and pigments, and there are also dust byproducts from municipal refuse.

The probability of occurrence of a dust explosion in any system of interest is the product of the probability of two events or conditions that are usually independent of one another. The first condition involves the presence of a significant flammable volume within the system; that is, dust must be present at a dispersed or dispersable concentration that is above its lean limit of flammability. The second condition involves the presence of an energy source within that flammable volume that is of sufficient magnitude to initiate a combustion wave. Both conditions are necessary for an explosion to take place. Frequently, popular accounts tend to emphasize the ignition event as the "cause," unjustifiably ignoring the conditions that generated the flammable volume in the first place.

[5]Underlined numbers in parentheses refer to items in the list of references at the end of this report.

Recent investigations attempting to quantify the first condition in terms of the composition limits of flammability of dust clouds have already been reported (13, 16-17). The present study deals primarily with the second problem: the ignition probability, with emphasis on the thermal ignition probability, which is simply quantifiable in terms of the autoignition temperature (AIT) and its dependence on the type of dust, concentration, and particle size. Some of the thermal ignitability data were presented previously (6-7, 15), but the present paper contains a more detailed discussion of the apparatus and more comprehensive data.

It is important to define the term "thermal ignition" as it is used in this report since the term "ignition" is used rather loosely in the combusion literature. As used here, the term "thermal ignition" refers only to the autoignition and explosion of a dust cloud caused by its intrinsic reactivity at an elevated temperature. This paper does not discuss the slow self-heating of dust layers or piles leading to their smouldering and eventual ignition into a diffusion flame or fire. This self-heating of a dust layer occurs on a much longer time scale and usually at a lower temperature than the thermal autoignition of airborne dust clouds. Also, the term "thermal ignition" is not used to describe any localized heating by an ignition source such as an electric spark even though a temperature could be associated with such an ignition source. Where data are presented for such a localized, electrical source, they are given in terms of the ignition source energy, not temperature. The term "thermal ignition temperature" as used in this report refers only to the initial temperature of the entire volume of the dust cloud.

Some preliminary data will also be presented on the conditions for the combined thermal and electrical ignition of Pittsburgh Seam coal dust. Such ignitability domains are readily delineated in the thermodynamic state-space of temperature versus composition. It is readily seen that those ignitability domains are contained within, and simply related to, the domain that defines the limits of flammability. Once the ignitability and flammability domains are delineated and their relationships clearly established, it becomes self-evident why such fundamental measurements are essential for a realistic evaluation of the practical explosion hazards in industrial and commercial establishments.

ACKNOWLEDGMENTS

The authors wish to acknowledge the important contributions of the following present and former staff members of the Pittsburgh Research Center (PRC): F. T. Duda, electrical engineer, for his valuable assistance in the design and construction of the 1.2-L furnace; G. Fetters and M. McGinnis, both engineering technicians, for their assistance in data collection; A. Bruszak, chemist, and F. Ambrose, physical science technician, for their contributions to the development of the rapid-sampling system for full-scale explosions; and D. Ng, research physicist, for the scanning electron microscope analyses.

APPARATUS AND EXPERIMENTAL METHOD

GODBERT-GREENWALD FURNACE

In the past, the Godbert-Greenwald furnace (8, 11) was part of a variety of laboratory test equipment used for evaluating the explosibility of dust clouds. This furnace (fig. 1) consists of a 3.9-cm-diameter vertical Alundum[6] tube, 23 cm long. Its volume is about 0.27 L. The top of the tube is connected by a glass adapter to a small brass chamber, with a hinged lid for inserting the dust. The solenoid valve between the dust chamber and an air dispersion tank (150 cm^3) controls the dispersion of the dust. The dust contained in the dispersion chamber is blown in through the top of the furnace. Ignition is indicated by the visual observation of flame coming out through the open bottom. The data obtained from such experiments are now included in standard reference tables (27). Since the dispersed dust cloud is not completely confined within the furnace, its concentration is not accurately known, as noted in an earlier publication (26). Two other problems associated with the open-bottom furnace are the short residence time for the dust in the high-temperature zone and uncertainty as to vertical temperature uniformity.

[6]Reference to specific products does not imply endorsement by the Bureau of Mines.

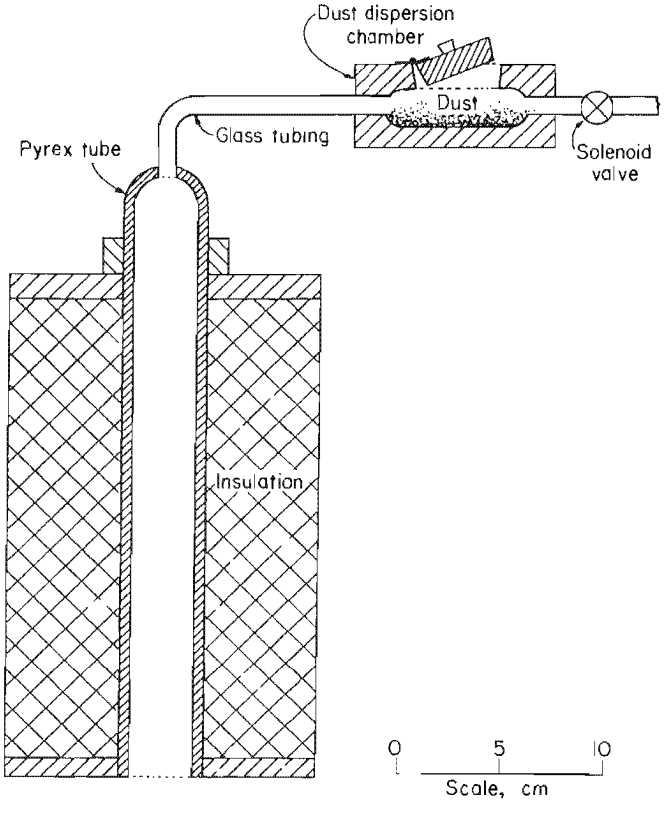

FIGURE 1. - Godbert-Greenwald furnace formerly used to evaluate thermal ignitability of dust clouds.

IMPROVED 1.2-L FURNACE

To correct for the dust dispersion uncertainty in the Godbert-Greenwald furnace and to improve on the visual criterion used to judge ignition, an improved furnace system was developed (6). The new system consists of a 1.2-L volume, coupled to an improved dispersion system. Figure 2 shows the furnace and associated instrumentation; the insulated furnace is in the center of the photograph, and the experimenter is holding the dust dispersion receptacle. A schematic of the furnace and dispersion receptacle is shown in figure 3. The ceramic combustion chamber is made of magnesium aluminum silicate and has inside dimensions of 10 cm diameter and 33 cm height. It is wrapped with a 9.7-m length of 18-gauge Nichrome heater wire. The axial temperature gradient within the furnace was reduced by concentrating the windings toward the ends. The heated chamber is insulated with a layer of ceramic, braided cloth. The final covering consists of a sheet metal shell 30 cm in diameter by 30 cm high, with a Transite top and bottom to hold the chamber in place. The remaining outer volume between the wrapped chamber and its outer covering is filled with loose ceramic insulation to reduce heat losses.

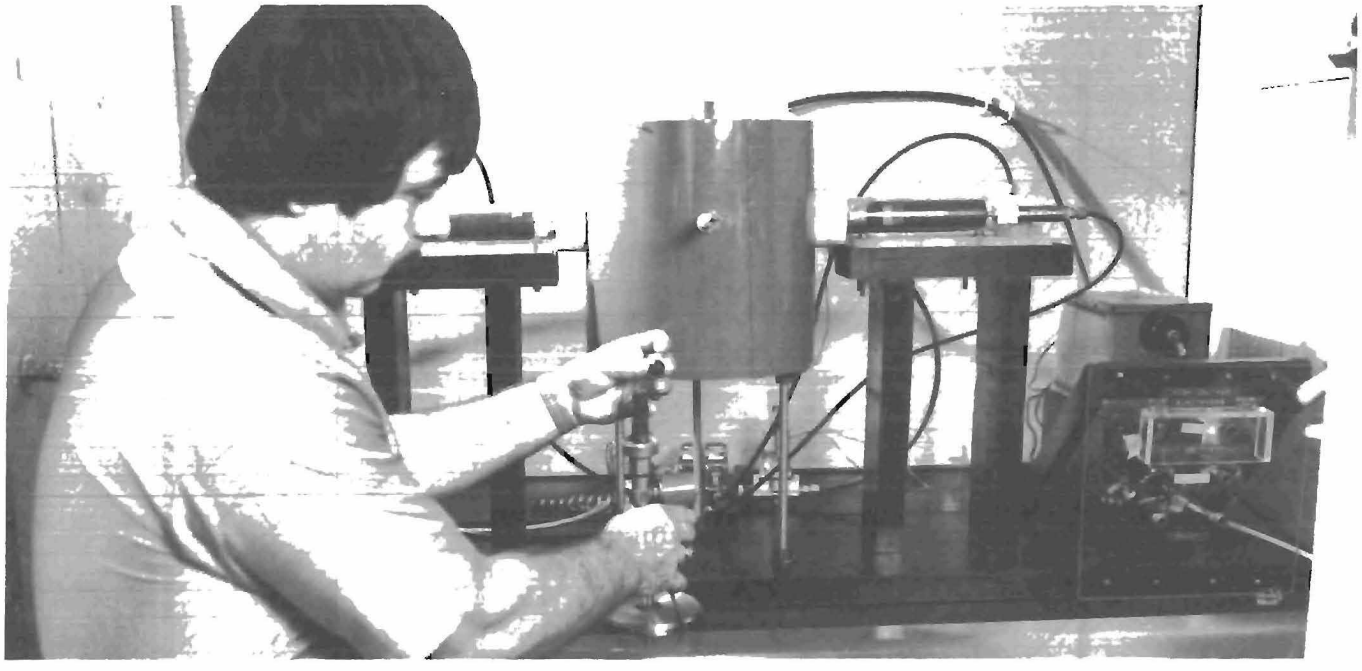

FIGURE 2. - The 1.2-L furnace used to study the thermal and electrical ignitability of dust clouds.

Four access holes pass through the furnace tube. Two are used for thermocouples: One is a 12.5-mil (318-μm) Chromel-Alumel thermocouple located at the wall of the furnace and used to control the furnace temperature; the other is a 1-mil (25-μm) platinum-rhodium thermocouple positioned in the center of the furnace to observe rapid changes in the temperature of the dust-air mixture during ignition. The remaining two holes are used either for spark electrodes or for a pressure transducer. It is also possible to use the holes for a rapid gas- and dust-sampling device that will be described later in this report.

As indicated earlier, the dust dispersion system was also improved. A detailed sketch of the new dispersion system is shown in figure 4, and data on its performance will be presented later in this section.

Data were obtained on the temperature distribution within the furnace by probing vertically along the furnace axis with a thermocouple, and the results are shown in figure 5. While the profiles show a fairly uniform temperature along the axis for most of the furnace volume, there are clearly convection currents that generate slightly higher temperatures in the upper half of the furnace. The very bottom of the furnace is significantly cooler than the central or upper portion. Since the lower temperature region near the bottom of the furnace is a small part of the furnace volume and since the temperature of the dust-air mixture is monitored continuously by a thermocouple during the dispersion and ignition process, it is felt that this temperature gradient does not significantly affect the experimentally measured ignition temperatures.

In normal operation, a diaphragm (glass microfiber filter) is placed over the top portion of the furnace. The dust to be tested is placed into the brass dispersion receptacle (fig. 4), which is then inserted into the bottom of the furnace, as shown in figure 3. With the

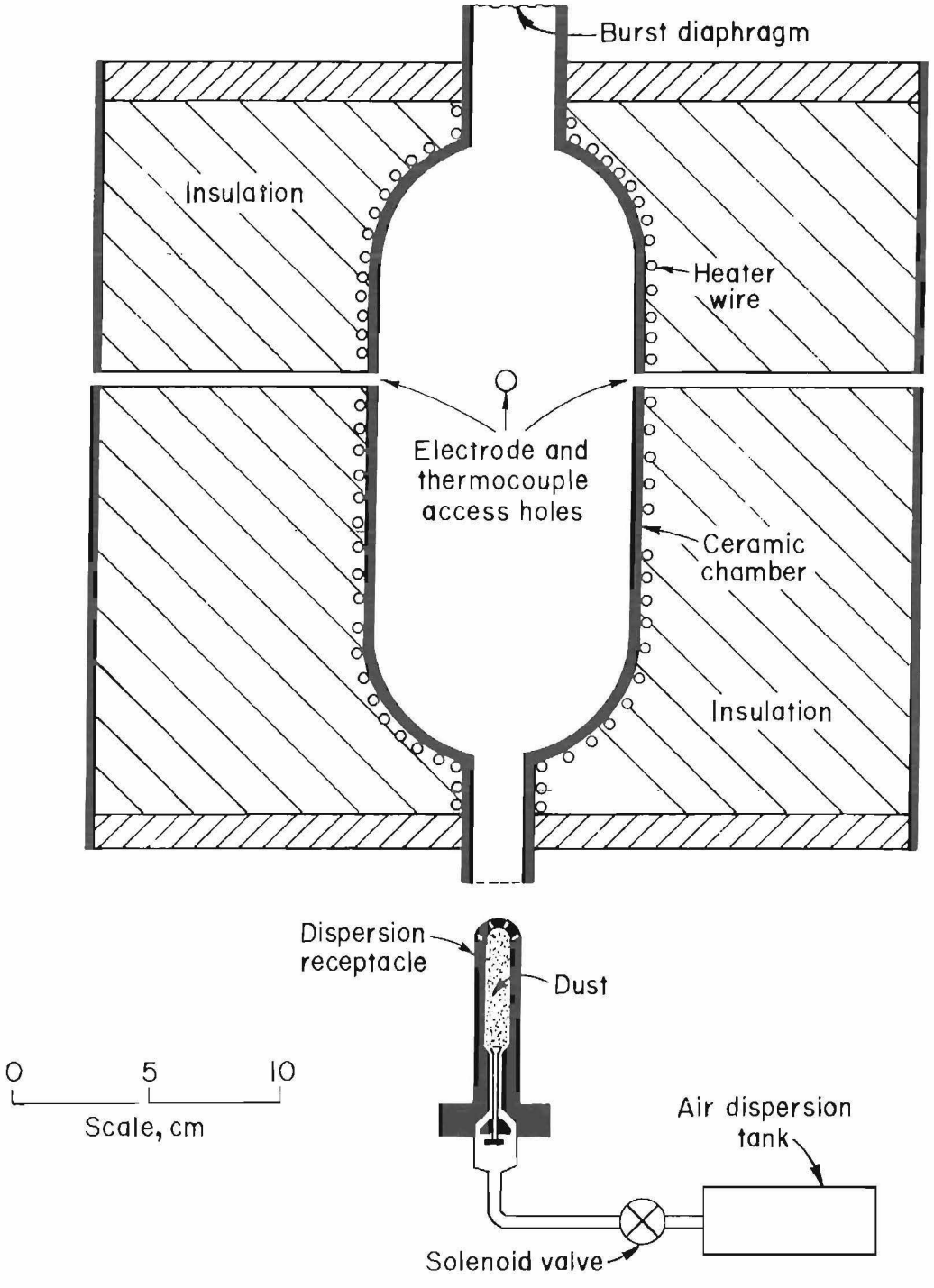

FIGURE 3. - Vertical cross section of 1.2-L furnace.

diaphragm sealing the top portion of the furnace and the dust injector in position, the furnace volume is essentially closed. The receptacle is fitted with a ceramic cloth sleeve, which insulates against the furnace heat and also functions as a seal after the receptacle is inserted into the furnace. The nozzle of the dust receptacle contains nine small (1.6-mm-diameter) holes through which the dust is ejected as fine jets; this process breaks up dust agglomerates formed in the dispersion receptacle. In the experiments, the dust receptacle is inserted into the heated furnace only moments before the sequence of ignition

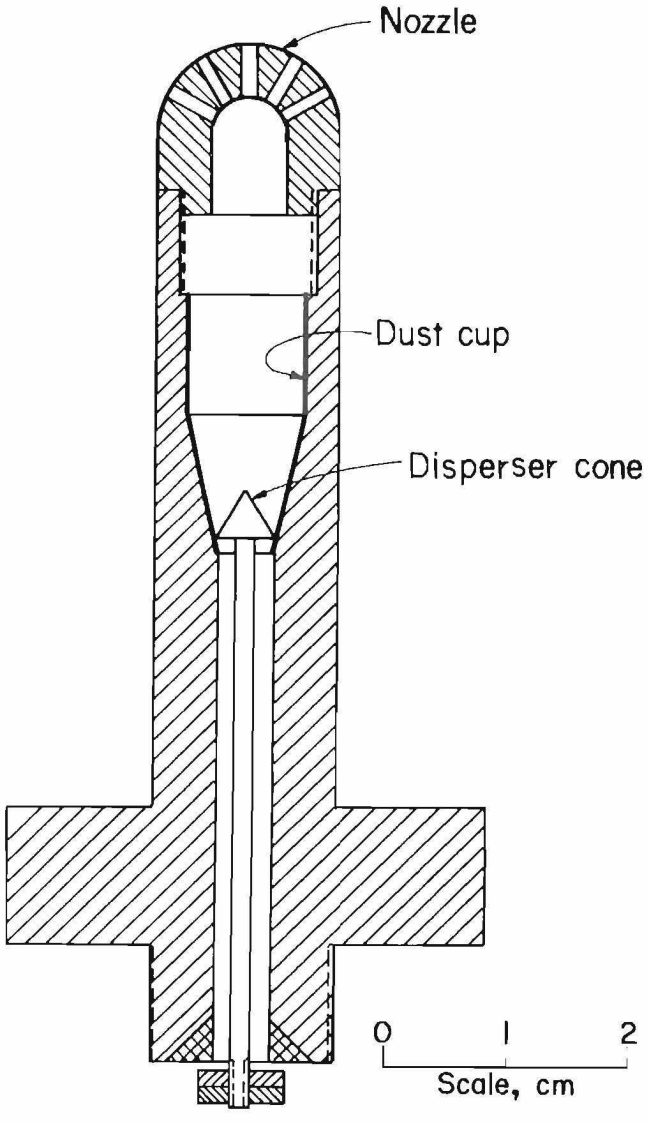

FIGURE 4. - Detailed drawing of dispersion receptacle.

events begins. This minimizes the effects of the furnace preheating the dust while it is in the dispersion receptacle. The air dispersion pulse is on for 30 msec, allowing approximately 60 cm^3 of air from a reservoir initially at 3.8 bar to disperse a uniform dust cloud into the furnace. Depending on the experiment, the maximum possible time the dispersed dust is exposed to the oven temperature is at least several seconds before the dust would settle by gravity.

A miniature optical dust probe (4-5) was used to measure the uniformity of the dust cloud and the effectiveness of the dispersion. The probe (fig. 6) consists of a light-emitting diode (LED) and a silicon photodetector that measures the

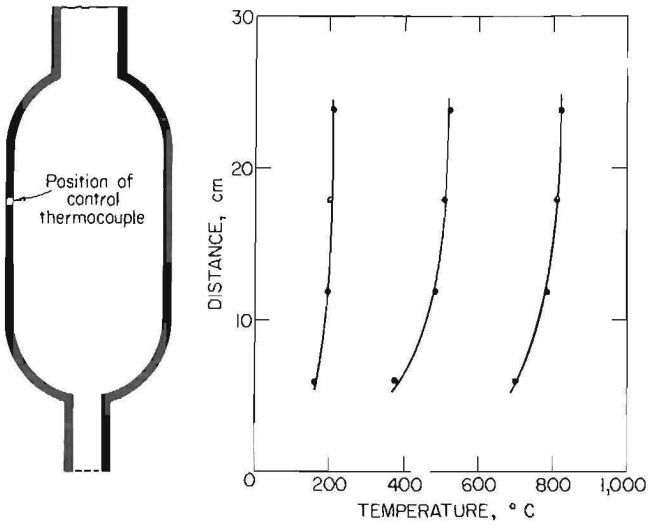

FIGURE 5. - Vertical temperature profile of 1.2-L furnace.

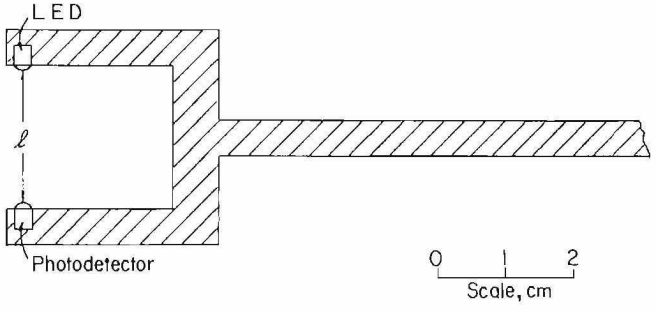

FIGURE 6. - Single-path-length optical dust probe.

transmission of light through a 1.8-cm path length (ℓ) in the dust cloud.

A typical recorder trace for the optical dust probe is shown in figure 7. The dust used in this test was Purple K fire extinguishant powder, which is specially fluidized so that it readily disperses as single particles. Initially, before dust dispersion, there is no attenuation of the light source. After dispersion of the dust, the transmission rapidly reaches a given level determined by the mass concentration of the dust and its particle size. As can be seen from the trace, the dust remains suspended at a relatively constant concentration for a time scale of the order of seconds. That time scale is long compared to the characteristic ignition delay times.

More detailed data on the uniformity of dispersion are shown in the

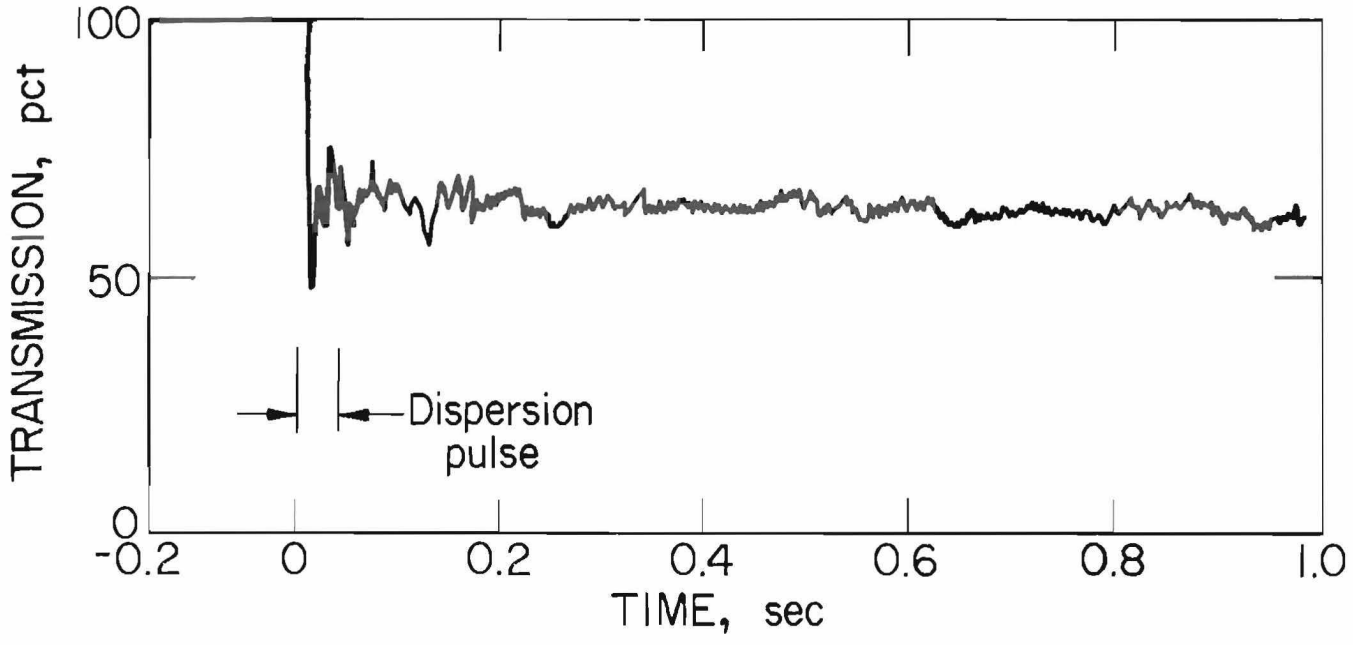

FIGURE 7. - Recorder trace of optical dust probe transmission.

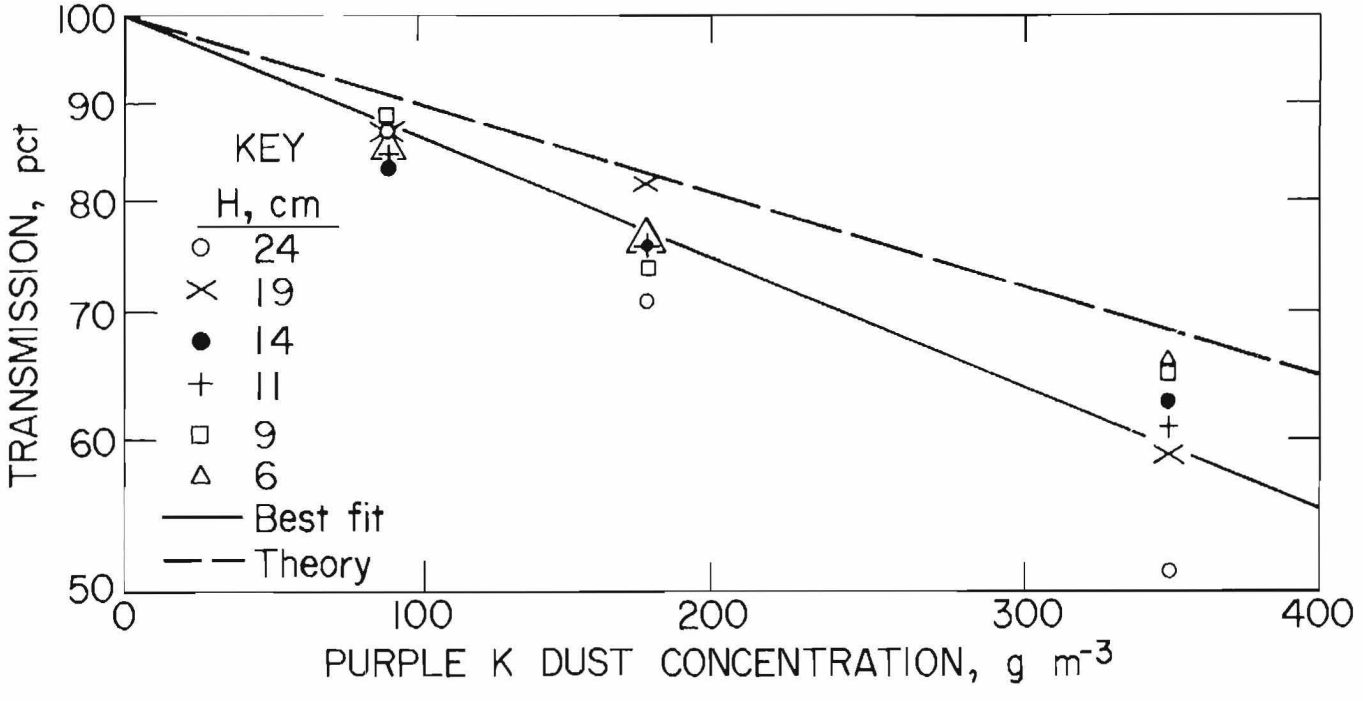

FIGURE 8. - Dust dispersion uniformity in 1.2-L furnace.

semilogarithmic plot of figure 8, where transmission measurements were made along the furnace chamber axis at a number of heights (H) from the chamber base. Purple K dust was used for these tests because it does not significantly coat the LED and detector windows. The probe transmission data show that the dispersed dust is fairly uniformly distributed along the entire height of the furnace. The theory curve shown in figure 8 is the transmission curve calculated from the Bouguer-Beer-Lambert law, which is

$$\tau = \frac{I}{I_o} = \exp(-QnA\ell) = \exp\left(\frac{3QC_m\ell}{2\rho D}\right), \quad (1)$$

where τ is the light transmission or ratio of transmitted intensity I to incident intensity I_o, Q is a dimensionless extinction coefficient, n is the number density of particles, A is the cross-sectional area of a particle of diameter D, ℓ is the path length, C_m is the mass concentration of particles, and ρ is the density of the solid particle. (A detailed discussion of the theory and calibration of the dust probe is found in reference 4.) The concentration value plotted is the mass of dust loaded into the dispersion receptacle divided by the volume of the furnace. The measured transmissions are systematically lower than the theoretical line because of a small dust coating on the windows of the LED and the detector. The data in figure 8 show clearly that the dispersion system is effective in generating a fairly uniform cloud of dust.

Several frames taken from a high-speed motion picture of the dust dispersion system in operation are shown in figure 9. The pictures show the formation of a coal dust cloud as it is being dispersed into a 10-cm-diameter glass vessel. The cloud would eventually reach a uniform concentration of 350 g m^{-3}. In the first frame, the ceramic furnace dimensions are shown by a dotted line for comparison. Although these pictures were taken of the disperser operating by itself outside the furnace, they confirm

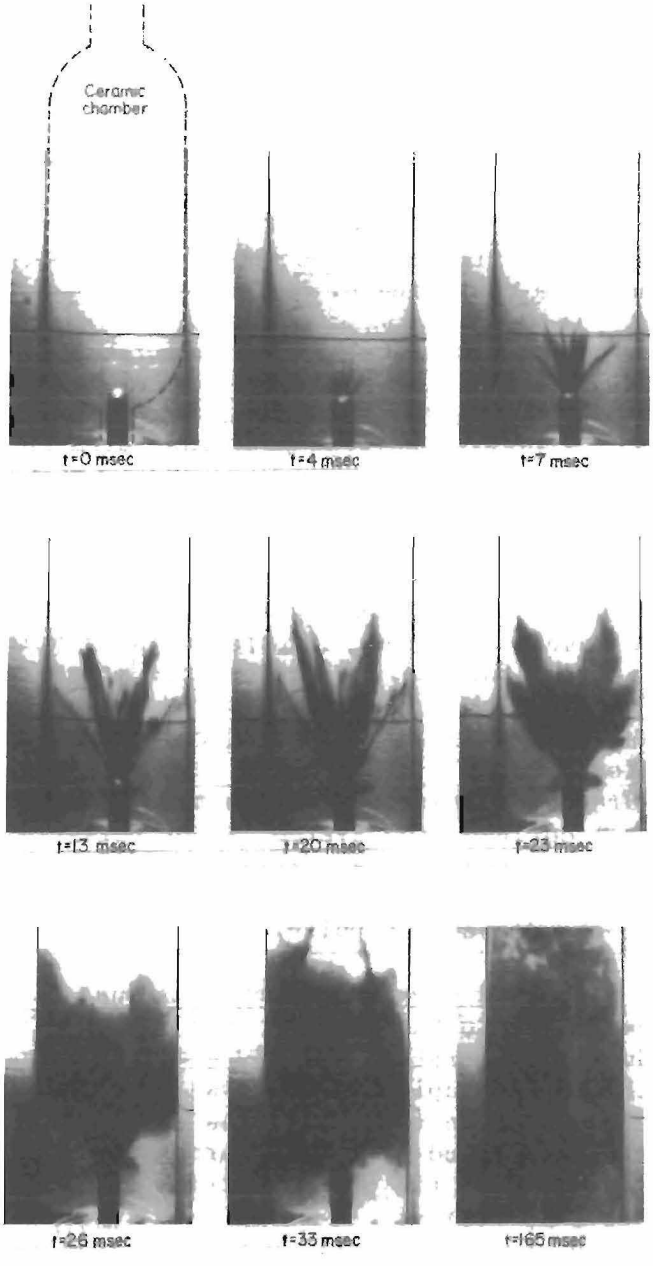

FIGURE 9. - Frames from high-speed motion picture of dust dispersion.

the effectiveness and uniformity of the dispersion system.

A burst diaphragm consisting of a glass microfiber filter that can withstand the high furnace temperature is used to seal the top portion of the furnace (fig. 3). The criterion for ignition in the thermal ignitability tests is both the rupture of that diaphragm (at 0.1 to

0.3 atm overpressure) and the emission of flame from the top of the furnace. Figure 10 shows high-speed photographs of a typical ignition at a furnace temperature of 800° C and a dust concentration of 130 g m^{-3}. The pictures clearly indicate the criterion used for ignition. Figure 10A shows rupture of the diaphragm. Figures 10B-C show flame ejecting from the furnace.

Figures 11-14 are various absolute pressure-time and temperature-time traces for different initial furnace conditions. The temperatures are measured with the 1-mil thermocouple in the center of the furnace. The thermocouple trace in figure 11 shows relatively no change in the initial furnace temperature of 500° C when an air pulse (without dust) is released from the dispersion receptacle into the furnace. The absolute pressure trace shows a slight pressure rise from the dispersion pulse owing to the addition of 0.06 L of cold air into the 1.2-L furnace. Clearly, although the volume is well defined, the system is not perfectly sealed because the pressure returns to its initial value shortly after the end of the dispersion pulse.

Figure 12 shows data for coal dust dispersed into the furnace at 500° C. The dust concentration was 130 g m^{-3}. Again, the thermocouple trace shows very little change in the temperature as the air and the dust cloud fill the furnace chamber. However, now the pressure trace initially shows a slight decrease in pressure caused by the larger mass of injected dust cooling the furnace. (The slight decrease in the pressure trace was significantly decreased when a preheated dust (aluminum oxide) was injected into the furnace under similar conditions.) In the coal dust case shown in figure 12, the furnace temperature is below the autoignition temperature of the dust so there is no ignition for this test.

A 93 msec

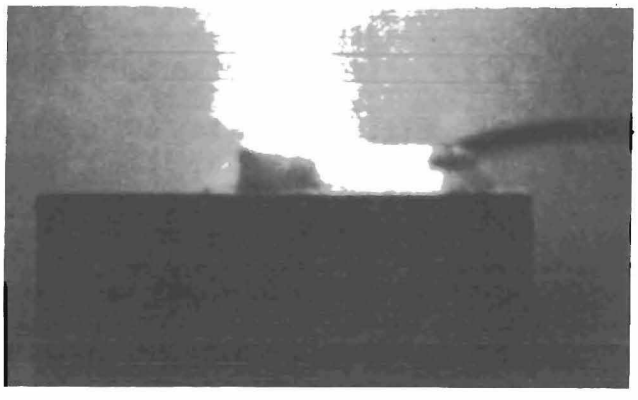

B 96 msec

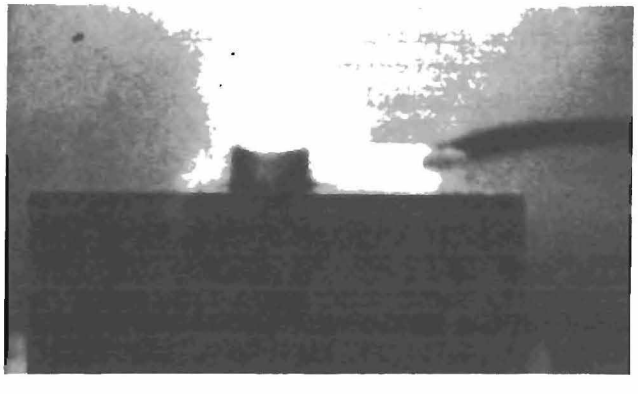

C 99 msec

FIGURE 10. - Frames from high-speed motion picture of a cool dust ignition at 800° C.

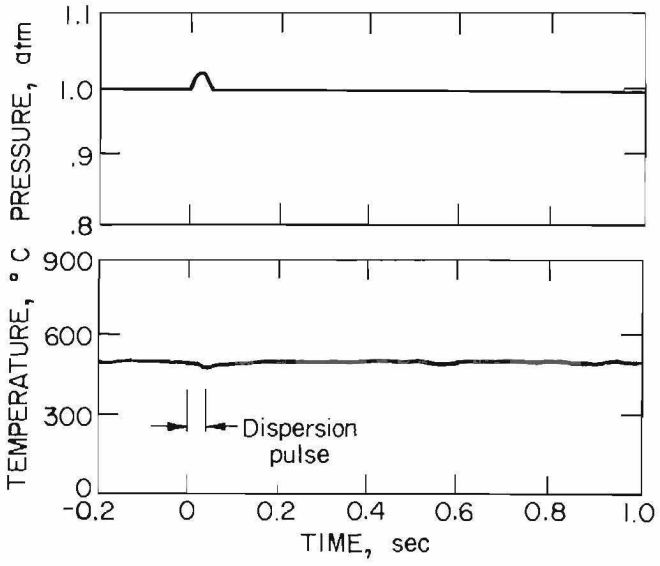

FIGURE 11. - Temperature and absolute pressure traces of the dispersion air pulse at furnace temperature of 500° C.

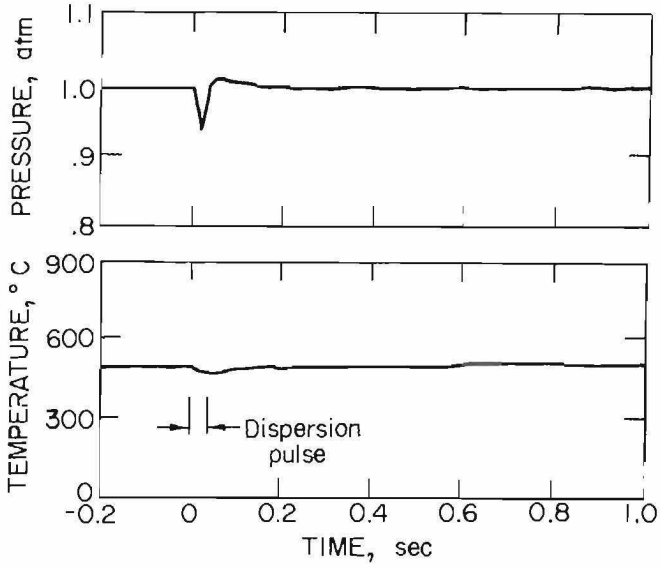

FIGURE 12. - Temperature and absolute pressure traces of a nonignition of dust cloud at 130 g m^{-3} and 500° C.

Figure 13 shows the pressure and thermocouple traces as a function of time for the same 130 g m^{-3} at a furnace temperature of 600° C. The thermocouple trace shows a drop in temperature as the dust and air enter the furnace. The temperature soon reaches the initial furnace temperature, and after a 0.9-sec delay there is a rapid increase in temperature, indicating ignition and explosion of the dust and air mixture. The pressure trace again shows a small initial drop in pressure as the dispersion pulse cools the furnace. This is followed by a sharp spike at the time of ignition. The rapid pressure decrease after peak pressure is due to the diaphragm rupture and resulting venting process, which generates a rarefraction wave, which cools the products.

A more rapid ignition at the higher furnace temperature of 800° C with the same 130-g m^{-3} concentration is shown in figure 14. Again we see a drop in pressure and temperature as the dust and

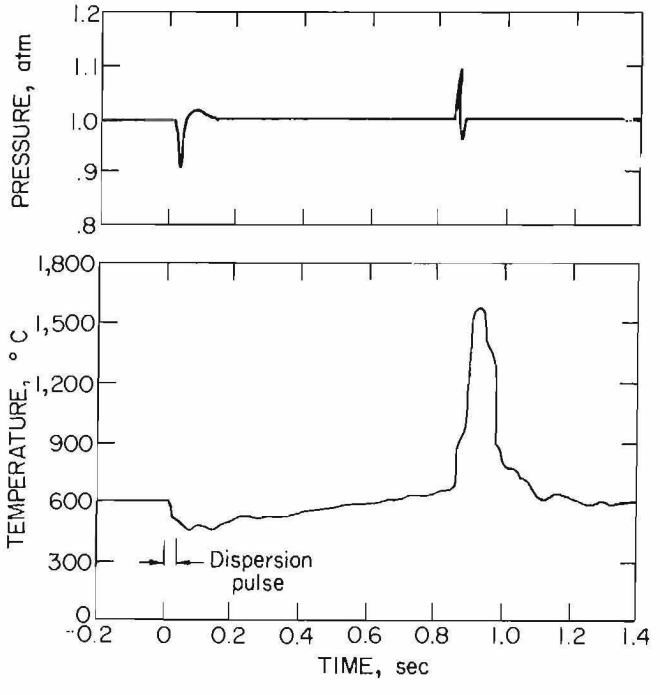

FIGURE 13. - Temperature and absolute pressure traces of an ignition of dust cloud at 130 g m^{-3} and 600° C.

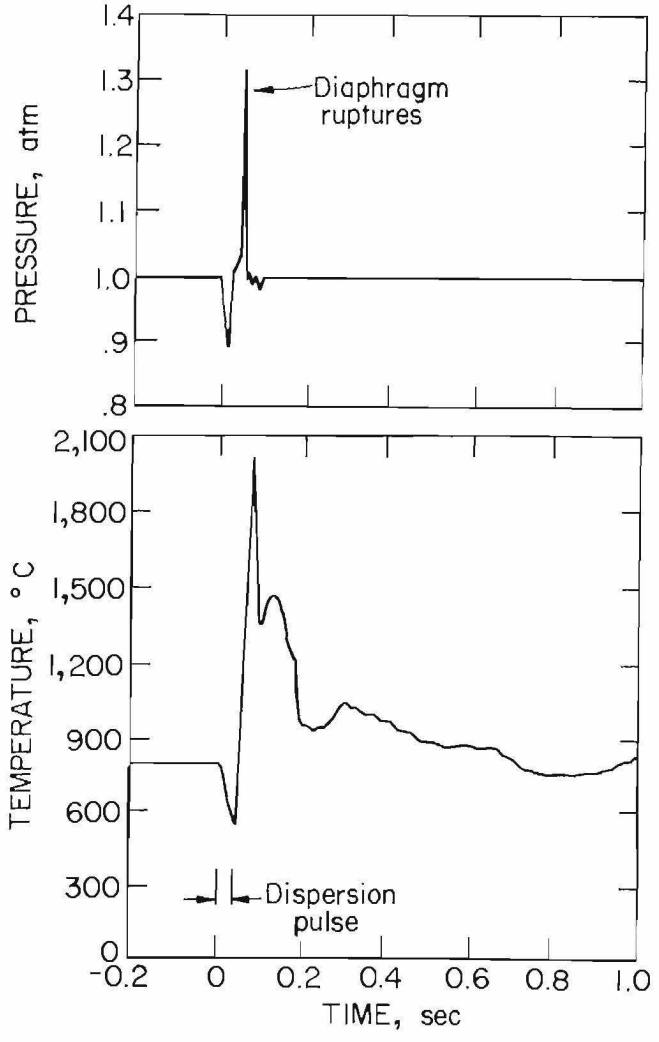

FIGURE 14. - Temperature and absolute pressure traces of a rapid ignition of dust cloud at 130 g m^{-3} and 800° C.

air are injected into the furnace, but now ignition occurs even before the dust cloud reaches the furnace temperature. The maximum thermocouple temperature before venting occurred was over 2,000° C. Again the pressure trace shows a very sharp rise in pressure at ignition, which is quickly quenched by the venting, which occurs at an overpressure of about 0.3 atm.

RAPID-SAMPLING SYSTEM

A system (7) was developed for the rapid grab sampling of heterogeneous mixtures of gases and dusts during the preignition and postignition stages of the experiments in the 1.2-L furnace. The furnace system is first fitted with a hypodermic sampling needle with its inlet end at the desired sampling point within the chamber and its sharp, injecting end protruding outside the chamber as depicted in figure 15. The sampling system is also shown in figure 2. Rapid sampling is achieved with a double-acting, air-pressure-actuated cylinder. The forward stroke of the cylinder thrusts the rubber septum seal of an evacuated glass sampling tube onto the protruding needle, which punctures the septum, filling the tube with gas and dust from the combustion chamber. The return stroke of the cylinder reseals the sampling tube by returning the mechanism to its original position.

A more detailed view of the mechanical device used to obtain rapid gas and dust samples is shown in figure 16. The main features of the system are a double-acting air cylinder (Bimba Manufacturing Co.) to power the sampling system, a piston section to which an evacuated glass collection tube is attached, and a sampling probe needle which feeds from the combustion chamber. A microprocessor controls a solenoid valve (not shown) which directs the air pulse to the double-acting air cylinder. In quantitative terms this rapid-sampling system is capable of sampling approximately 5 cm^3 (STP) of reacting gas together with its dust content in a time scale of the order of 30 msec.

A trimodal distribution of coal dust was used to test the particle-sampling efficiency of the rapid-sampling system

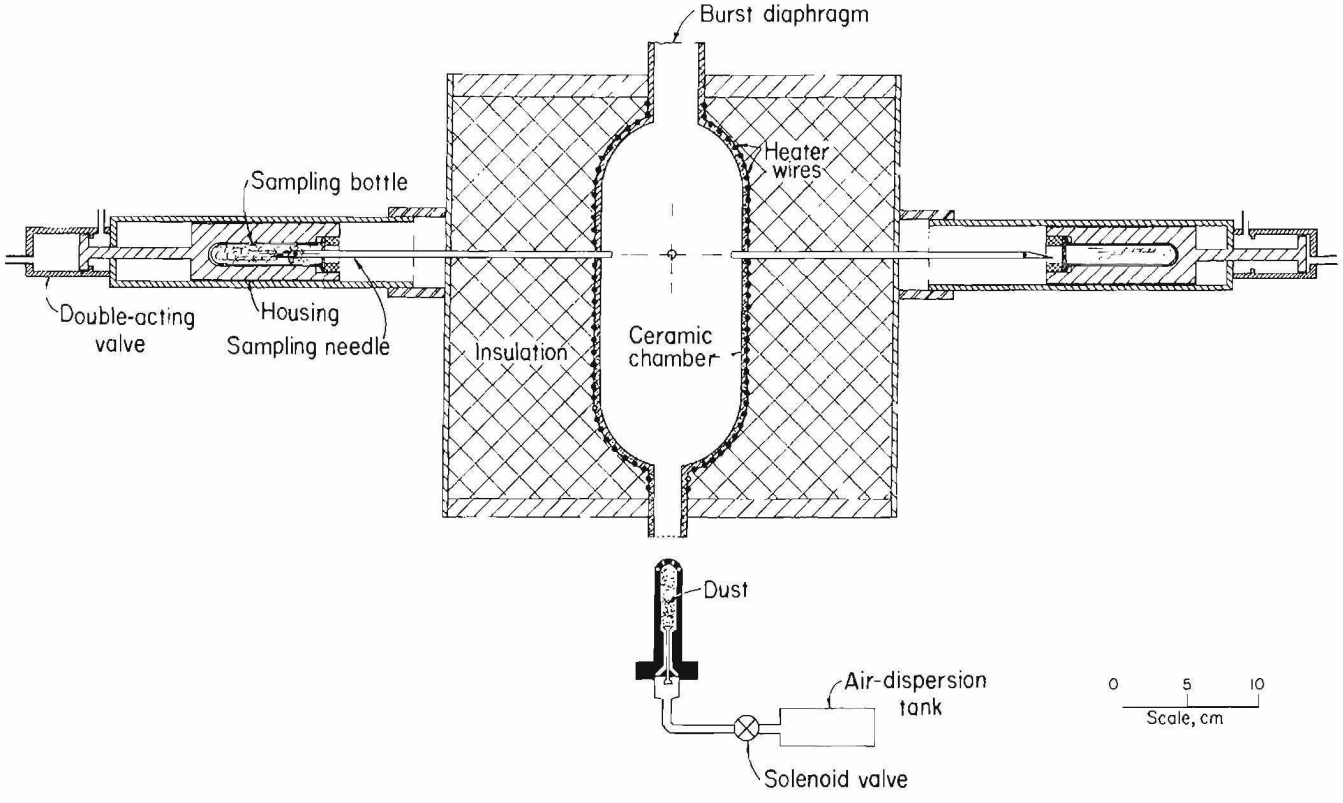

FIGURE 15. - Rapid sampling system coupled to 1.2-L furnace.

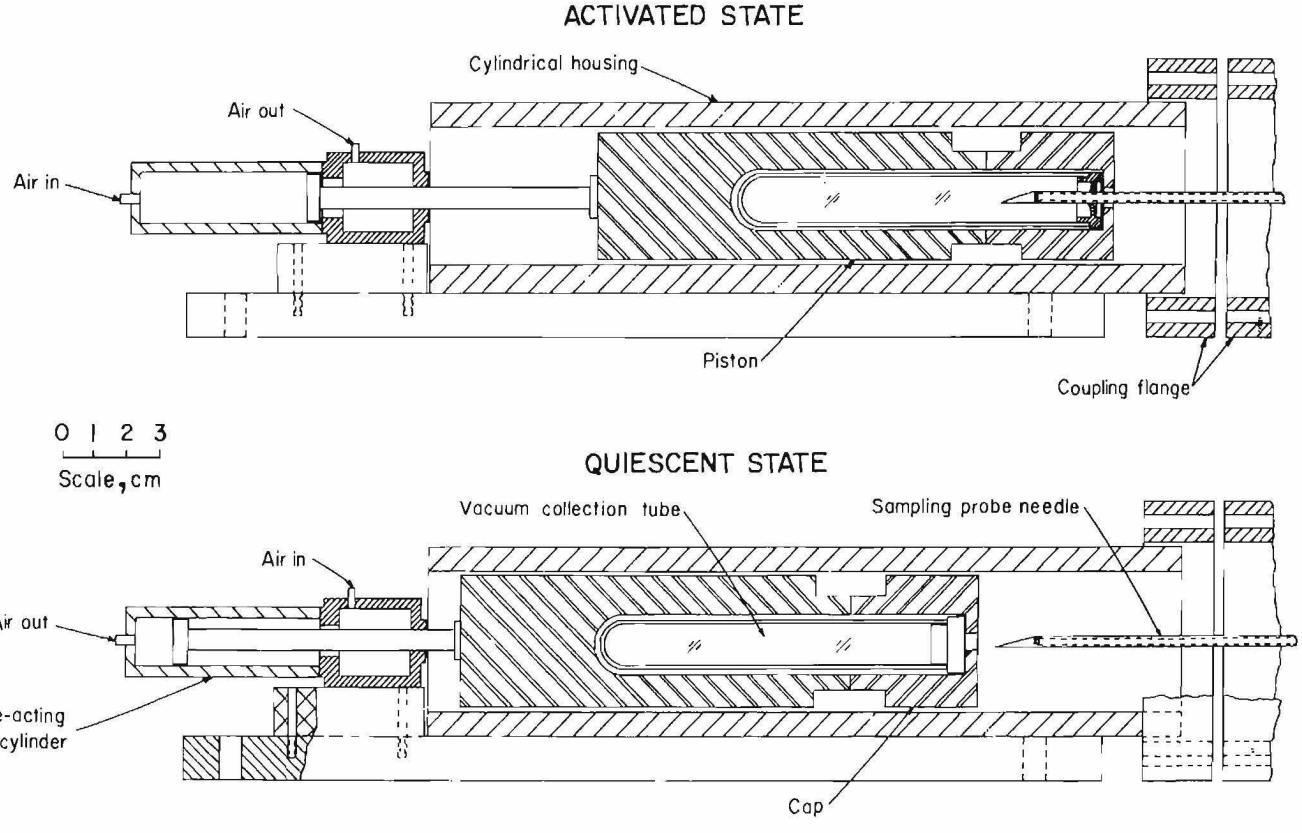

FIGURE 16. - Operational schematic of rapid-sampling system.

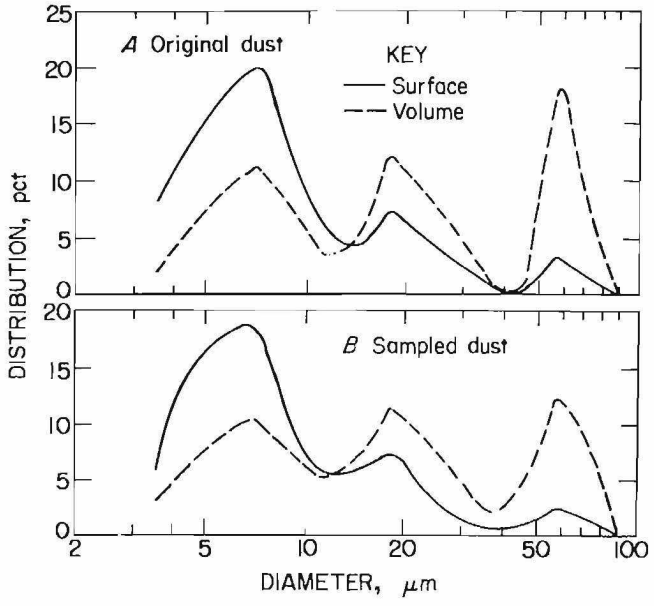

FIGURE 17. - Dust particle sampling efficiency observed with a trimodal size distribution.

interfaced with the 1.2-L furnace, and the data are shown in figure 17. The trimodal size distribution was prepared from a mixture of three sizes of coal dust with surface mean diameters of 5, 15, and 55 μm. The original and sampled dust size distributions were obtained with a Coulter counter (3) particle size analyzer. The size distribution of the original dust is shown in figure 17A. Figure 17B shows the results of a 110-msec sample of that dust dispersed in the 1.2-L furnace at room temperature. The accuracy of the Coulter counter is limited at the larger sizes because there were only a few large particles compared with the thousands of small particles in the collected samples. Within this size measurement accuracy, the data show that there is no significant size discrimination for sampled coal dust particles for sizes up to at least 70 μm in diameter.

THERMAL IGNITABILITY DATA FOR THE GODBERT-GREENWALD FURNACE

Before the 1.2-L furnace was built, some preliminary data were obtained with the Godbert-Greenwald furnace. Data are shown in figure 18 for Pittsburgh Seam bituminous coal with an as-received volatility (1) of 35 pct and for Pocahontas Seam bituminous coal with 16 pct volatility. Since the dust is unconfined at the bottom when it is injected into the furnace from the top (fig. 1), dust concentrations are not known. Accordingly, the ignition temperature is plotted as a function of the mass of dust blown into the furnace. Although the data for Pocahontas coal dust appear well behaved, there is an anomalous increase (dashed line in fig. 18) in the AIT for Pittsburgh coal dust at loadings in excess of 100 mg. The lowest AIT for either coal is about 625° C, which is comparable to values reported by earlier Bureau researchers (8, 25, 27) as the "minimum cloud ignition temperature" in the Godbert-Greenwald furnace. A detailed comparison of these data and the data from the new 1.2-L furnace will be presented later.

THERMAL IGNITABILITY DATA FOR THE 1.2-L FURNACE

The characteristics for the various dusts tested in the new, 1.2-L furnace are shown in table 1. The proximate analyses and heating values are by ASTM methods (1) and are for the as-received samples. The surface mean diameters, $\bar{D}_s$, and the volume or mass mean diameters, $\bar{D}_w$, were calculated from a size distribution measured by a Coulter counter (3). The measured size distributions for most of the dusts are shown in figure 19. The size-classified, narrow distributions are shown by the solid curves, and the broad distributions (minus 120 mesh) are shown by the dashed lines. The distributions shown do not include all distributions studied but are typical of those used. Each narrow distribution is characterized by its surface mean diameter, $\bar{D}_s$, which is shown as a short vertical line near the center of each distribution curve. All of the thermal ignitability tests for the dusts were made in air with 21 pct O_2.

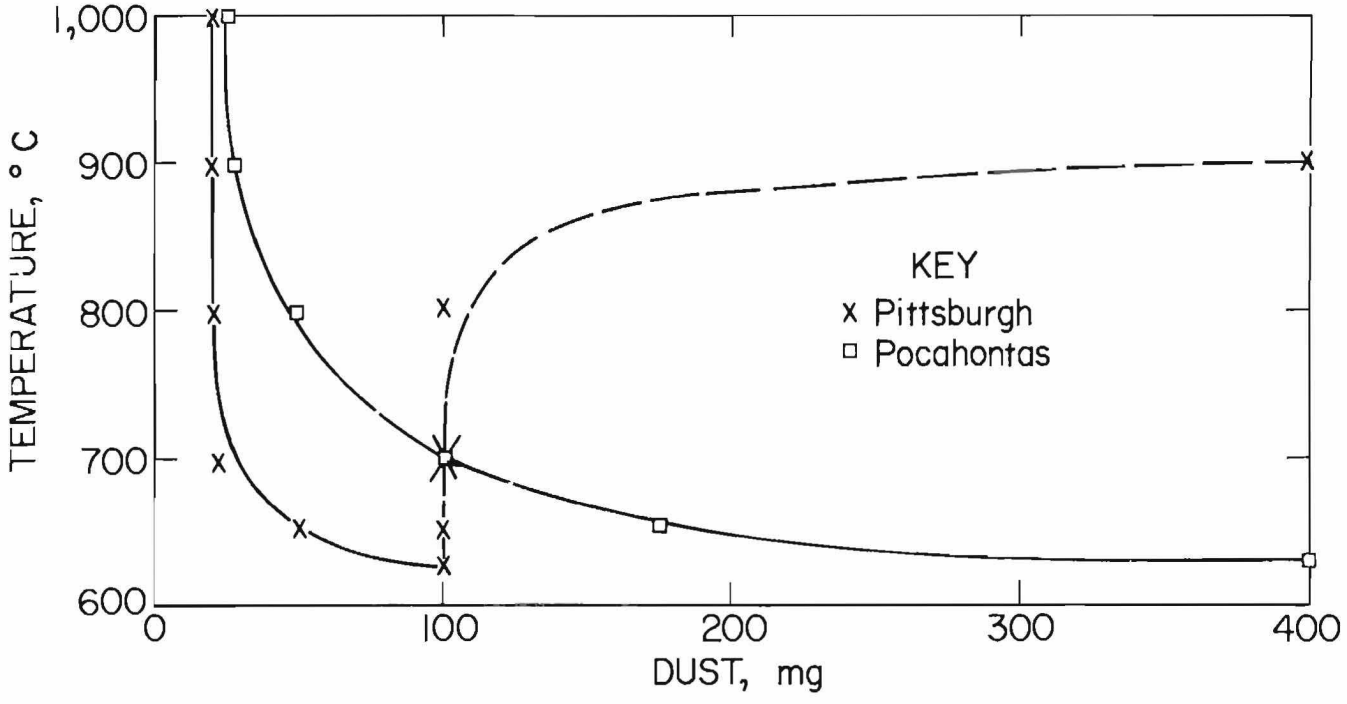

FIGURE 18. - Thermal ignitability data obtained with the Godbert-Greenwald furnace for Pittsburgh and Pocahontas coal dusts.

TABLE 1. - Proximate analyses, heating values, and sizes of various dusts

Dust	Mean diameter, μm		Proximate analysis, pact				Heating value, cal/g
	$\bar{D}_s$	$\bar{D}_w$	Moisture	Volatiles	Fixed carbon	Ash	
Bituminous coal:							
Pittsburgh Seam.....	(1)	(1)	1.6	35.0	56.1	7.3	7,460
Pocahontas Seam.....	(1)	(1)	.8	16.2	76.7	6.2	8,010
Subbituminous coal, western.....	~20	~41	10	34	47	8	5,730
Lignite, North Dakota.....	~27	~42	25	33	35	8	4,490
Anthracite, Reading, Pa...	5	9	.9	6.6	83.3	9.2	7,330
Gilsonite, Utah.....	15	34	.5	85.4	14.0	.2	9,870
Polyethylene.....	(1)	(1)	.0	99.5	.4	.1	11,090

[1]Various size distributions.

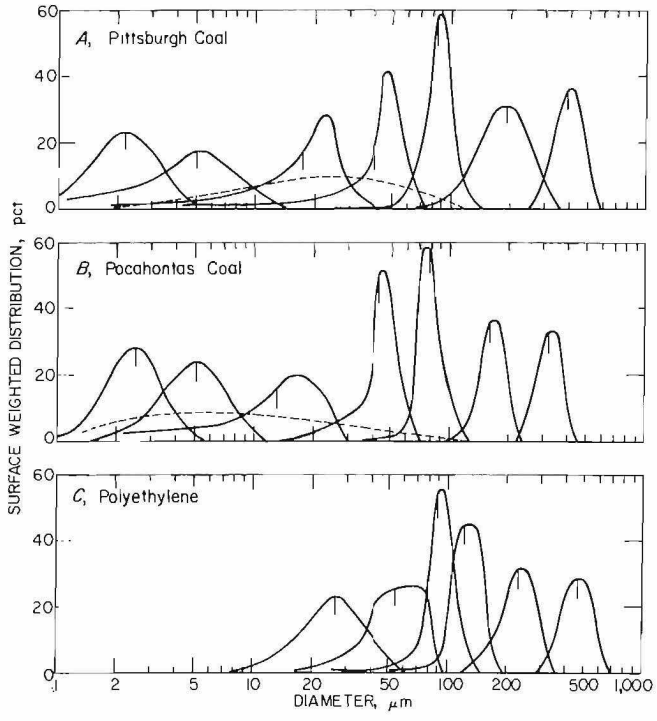

FIGURE 19. - Size distributions for two coal dusts and a polyethylene dust.

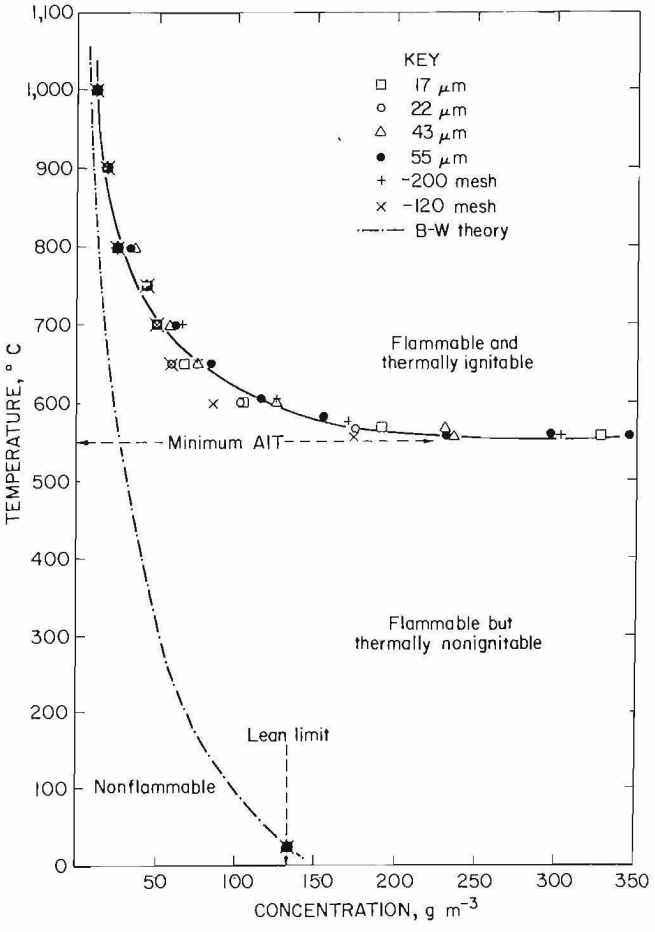

FIGURE 20. - Domain of thermal ignitability for four narrow and two broad distributions of Pittsburgh coal dust with $\bar{D}_s \leq 55$ μm.

PITTSBURGH SEAM BITUMINOUS COAL

The thermal autoignition data for various sizes of Pittsburgh seam bituminous coal dust (35 pct volatility) dispersed in the preheated 1.2-L furnace are shown in figure 20. The data points represent the boundary between ignitable and nonignitable concentrations at a given temperature. The concentrations are the actual concentrations, namely the mass of dust divided by the chamber volume. No corrections are included for the reduction in the mass concentration of air at the elevated temperatures. The minimum AIT is 560° C, a value that agrees closely with those reported for the vapors of solid aromatics such as anthracene, naphthalene, and biphenyl (32), which are similar to the tar volatiles generated from coal. The minimum value is approached asymptotically at the higher dust concentrations. The general shape of the curve for coal is similar to that observed for liquid hydrocarbons (20), although the absolute AIT values for the saturated hydrocarbons are much lower. The 560° C minimum AIT in the present apparatus for Pittsburgh coal is significantly lower than the value measured with the original Godbert-Greenwald furnace. The lower value may be due to the improved dispersion and longer residence time in the confined volume of the 1.2-L furnace and/or to the more uniform temperature and concentration distributions in the new system.

As concentrations are diminished to below 250 g m^{-3}, the ignition temperature increases very gradually at first; then, at compositions significantly leaner than stoichiometric, the curve steepens markedly. The lowest dust concentration that could be accurately weighed and dispersed is about 10 g m^{-3}.

The solid curve through the data points in figure 20 delineates the domain of thermal ignitability, and it is instructive to compare it with the flammability domain. The thermal ignitability curve defines the boundary at which a dust cloud will autoignite owing to its intrinsic reactivity at that temperature, without the need for any additional external ignition source. The flammability curve defines the boundary at which the dust cloud is capable of propagating a flame after a flame front has been initially established by such an external ignition source. The available data for most flammability limits show a temperature dependence given by the modified Burgess-Wheeler (B-W) theory (32):

$$L_T = L_{298}\,[1 - 0.000721(T-298)], \quad (2)$$

where L_T is the lean limit in volume-percent at temperature T (Kelvin) and L_{298} is the lean limit at room temperature. In terms of the mass concentration, C, of the fuel per unit volume, one obtains

$$C_T = C_{298}\left(\frac{298}{T}\right)[1 - 0.000721(T-298)]. \quad (3)$$

For Pittsburgh coal, the room temperature lean limit is $C_{298} = 130$ g m^{-3} as measured in an 8-L flammability chamber with a strong ignition source (13, 16). This limit value is the lowest concentration of air-dispersed dust that can sustain an explosion at ambient initial temperature and pressure. The chain-dashed curve in figure 20 is the B-W theory extrapolated from that room temperature limit value. It therefore delineates the domain of flammability in the same thermodynamic state-space of temperature and composition. Clearly the domain of thermal ignitability is always contained within

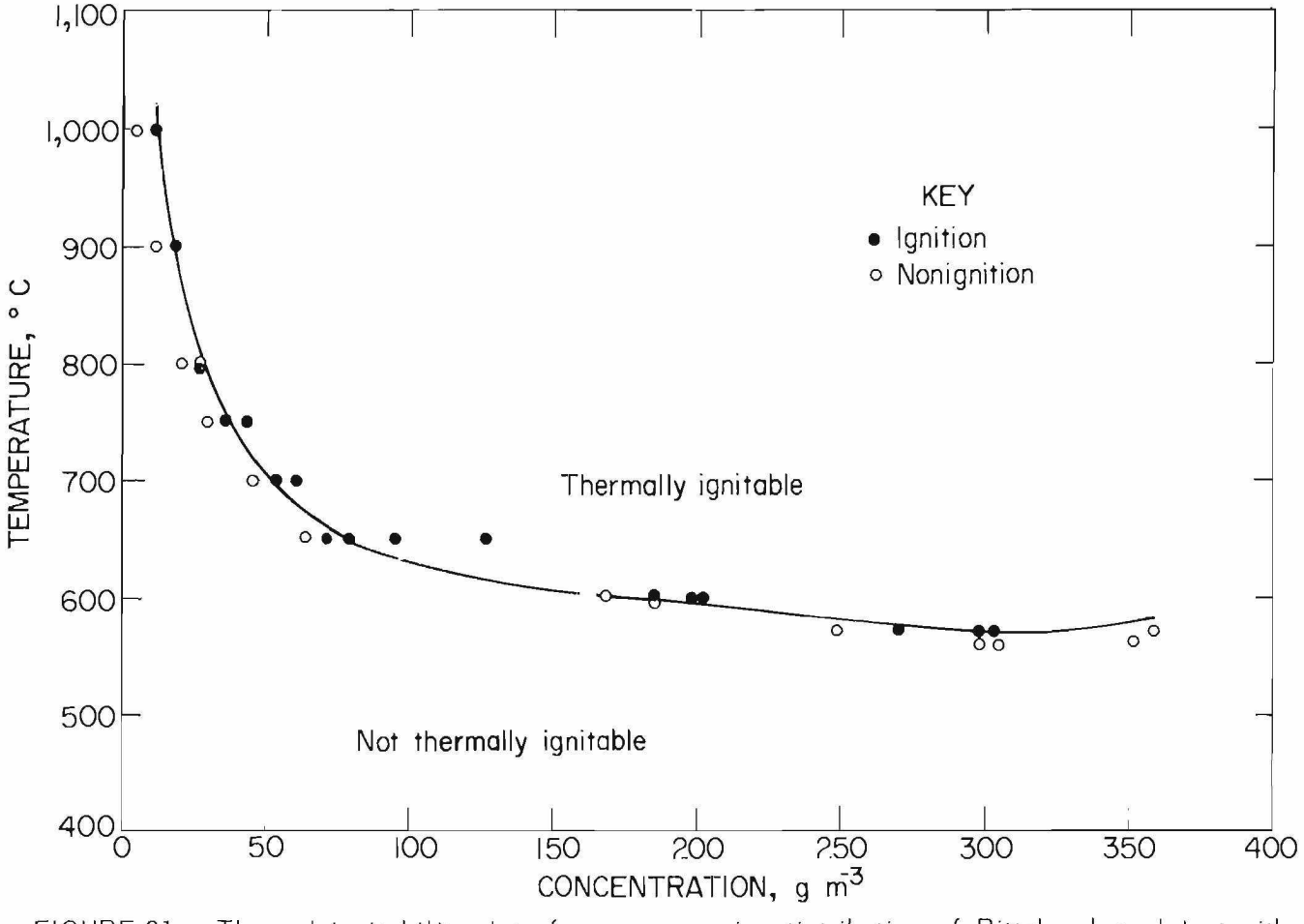

FIGURE 21. - Thermal ignitability data for a narrow size distribution of Pittsburgh coal dust with $\bar{D}_s = 17$ μm.

that domain of flammability. The two boundary curves approach one another only at elevated temperatures, where ignition appears to occur as soon as a lean limit composition is dispersed. At lower temperatures there is a large region between the two domains representing a range of cloud concentrations and temperatures that are flammable but not thermally autoignitable.

The data in figure 20 include six different size distributions. The four narrow ones have surface mean diameters, $\bar{D}_s$, of 17 to 55 μm. The two broad distributions were minus 200 mesh (with $\bar{D}_s$ = 22 μm and $\bar{D}_w$ = 31 μm) and minus 120 mesh (with $\bar{D}_s$ = 27 μm, $\bar{D}_w$ = 45 μm, and about 85 pct minus 200 mesh). The data show no systematic size dependence over this range. A similar insensitivity to particle size in that same size range was also observed for the room temperature lean limits (6, 15-17).

Figure 21 shows the detailed thermal ignitability data for the narrow size distribution of Pittsburgh coal dust with $\bar{D}_s$ = 17 μm and $\bar{D}_w$ = 21 μm. The data points show the actual ignitions and nonignitions for tests at various temperatures and concentrations. The minimum AIT is 565° C, and there is very little scatter in the data.

The data for a larger Pittsburgh coal dust with $\bar{D}_s$ = 55 μm and $\bar{D}_w$ = 62 μm are shown in figure 22. The data points still show very little scatter in the data. The minimum AIT is 560° C. Any small differences in the two curves of figures 21 and 22 are within the experimental errors of the measurements; hence it is concluded that the ignitability of Pittsburgh coal dust is independent of particle size for these smaller sizes.

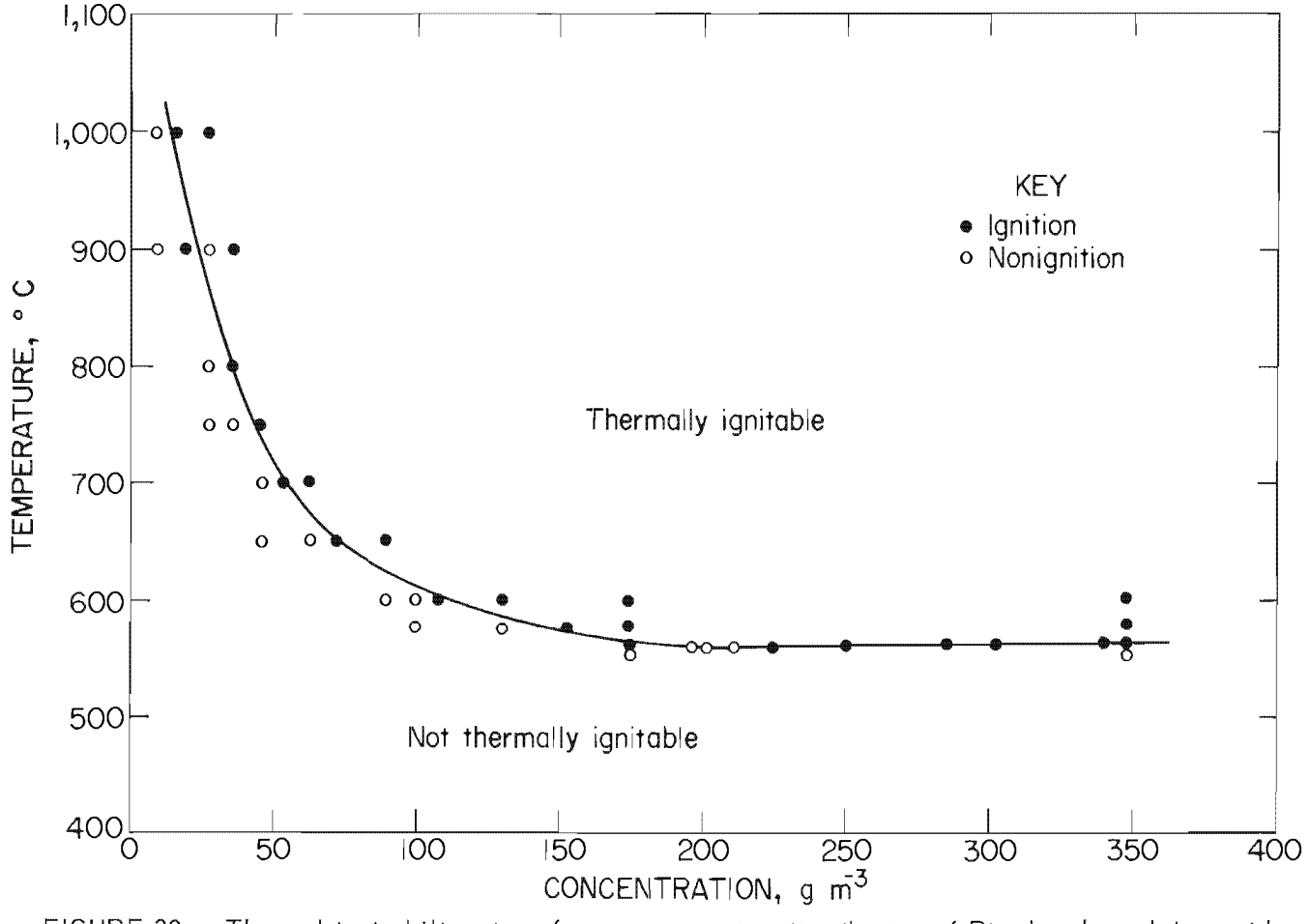

FIGURE 22. - Thermal ignitability data for a narrow size distribution of Pittsburgh coal dust with $\bar{D}_s$ = 55 μm.

A significantly larger size of Pittsburgh coal dust with $\bar{D}_s$ = 300 μm and $\bar{D}_w$ = 360 μm is shown in figure 23. The minimum AIT is now significantly higher, near 700° C. At this size, there is more scatter in the data points.

Figure 24 summarizes all the data obtained for the thermal ignitability of several large sizes of Pittsburgh coal dust and compares them with the 15- to 55-μm data curve taken from figure 20. The data points represent the boundary between ignitable and nonignitable concentrations at a given temperature.

The lean limit concentration and the AIT increase significantly for the coarser dusts. This size dependence of the AIT was also observed by Finney and Spicer (9) using a Godbert-Greenwald furnace. This particle size dependence above 55-μm diameter reflects a shift in the rate control of the overall process. The smaller particle sizes are under a gas-phase reaction rate control, whereas the larger sizes are under a devolatilization rate control. A detailed model of this type of combustion behavior was presented in references 15 and 17.

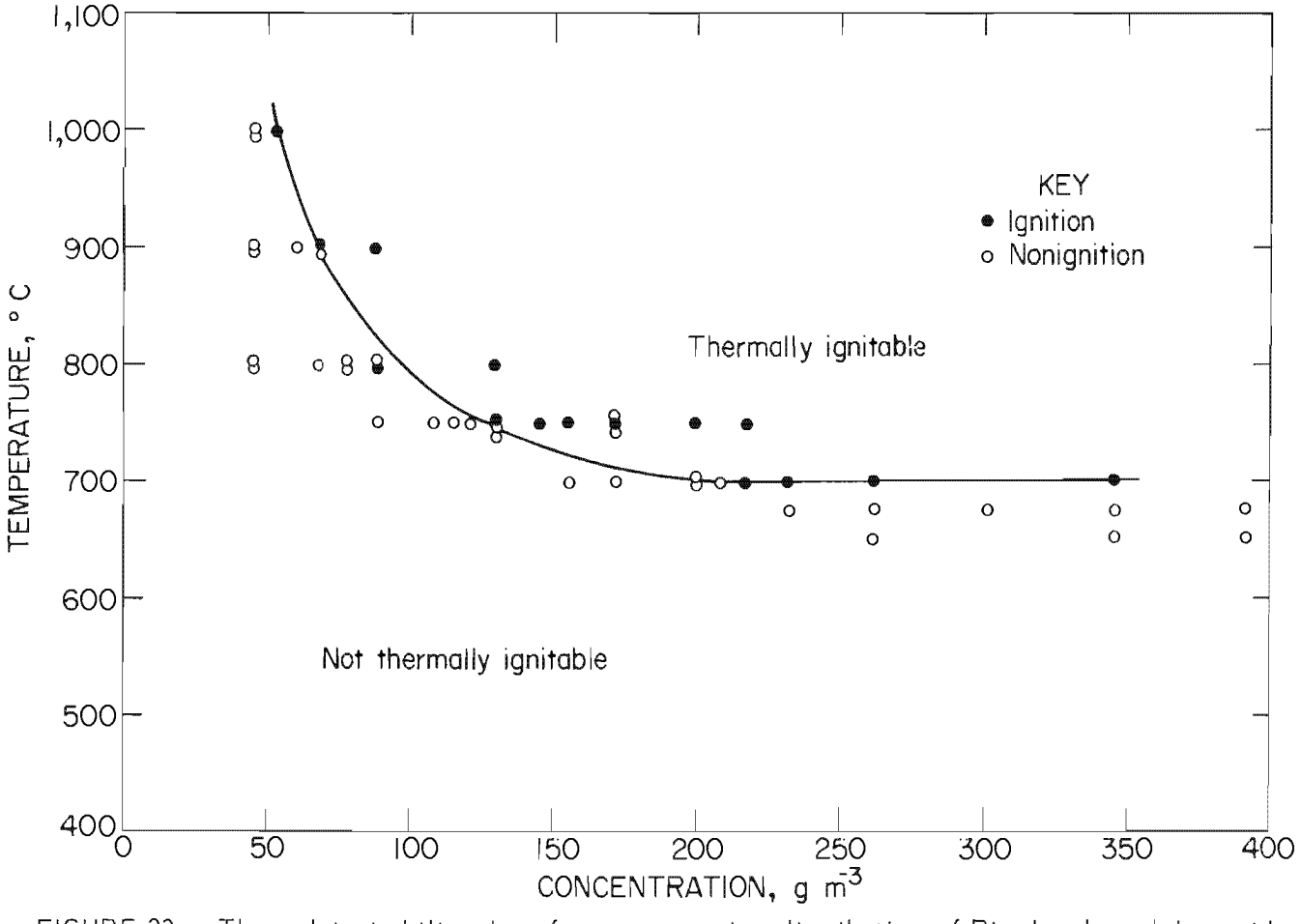

FIGURE 23. - Thermal ignitability data for a narrow size distribution of Pittsburgh coal dust with $\bar{D}_s$ = 300 μm.

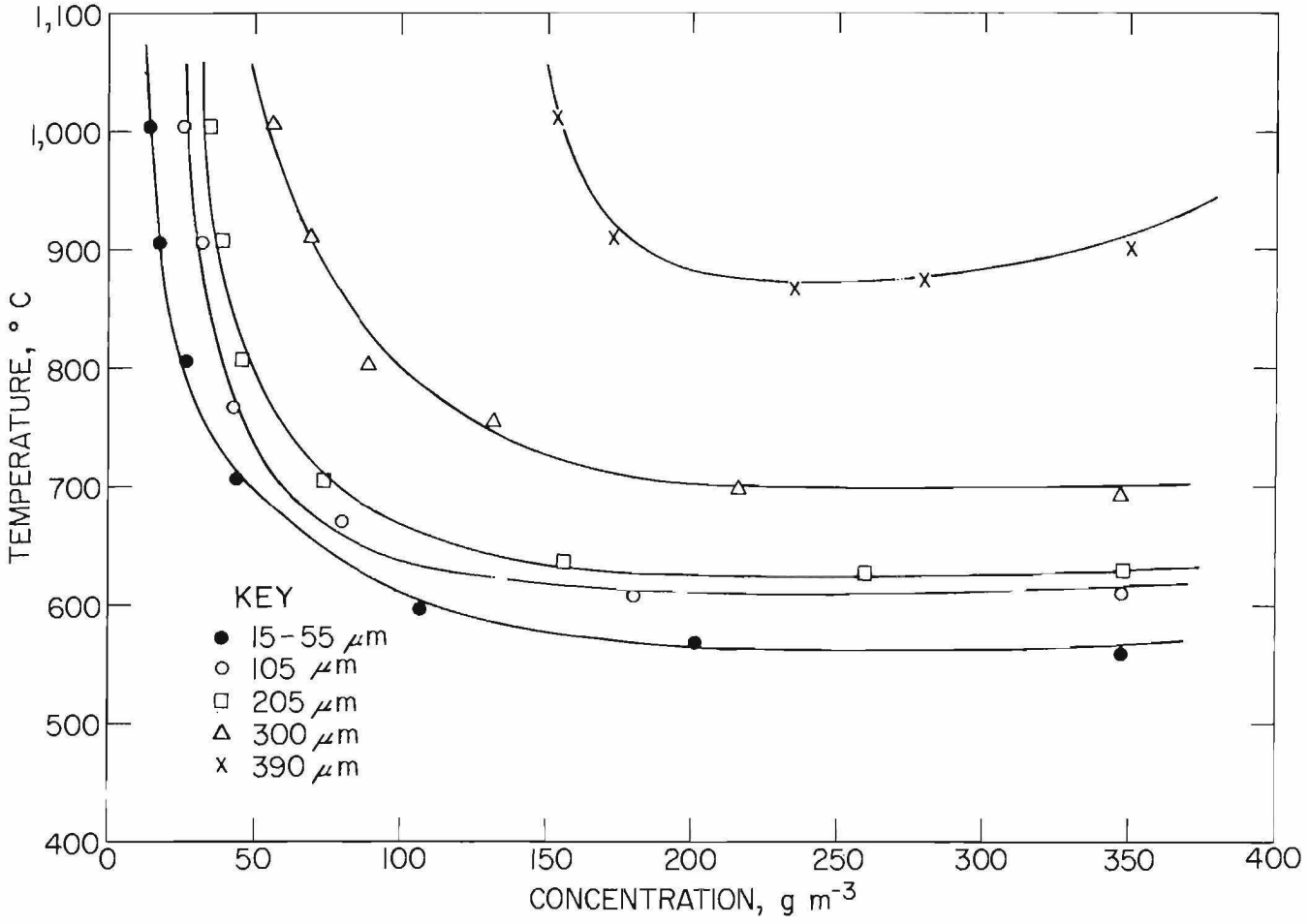

FIGURE 24. - Domain of thermal ignitability of several larger sizes of Pittsburgh coal dust compared with the thermal ignition curve for the smaller dusts ($\bar{D}_s \leq 55$ μm) from figure 20.

The curves shown in figures 20-24 for Pittsburgh coal are ignition temperature measurements as a function of coal dust concentration. Although the dust concentration per unit volume of air (21 pct O_2) in the furnace is the independent variable that is accurately controlled, it is important to recognize that each unit volume of air with which the coal reacts contains a lower mass concentration of oxygen as the furnace temperature increases. It is instructive to try to account for this changing oxygen content by transforming the mass concentration per unit volume scale to a mass ratio scale. The tranformation of figure 20 is made in figure 25. The ignition temperature data are now plotted as a function of the mass ratio of coal to oxygen in the furnace. Also shown in figure 25 is the lean limit curve, labeled B-W theory, which was previously shown in figure 20 and is now also transformed to the mass ratio scale. A stoichiometric ratio of whole coal to oxygen corresponds to a mass ratio of 0.4, and this is shown on the graph as the vertical line labeled S_c. However, as has been shown in previous publications (13, 15, 17), the important factor in determining the lean flammability limit of a carbonaceous dust is its combustible volatile content. Accordingly, the vertical line S_v corresponding to a stoichiometric ratio of Pittsburgh coal volatiles to oxygen is also shown at the mass ratio 0.9. This stoichiometric value for the volatiles was calculated from the measured amount of volatiles under rapid heating conditions (18). The room temperature lean

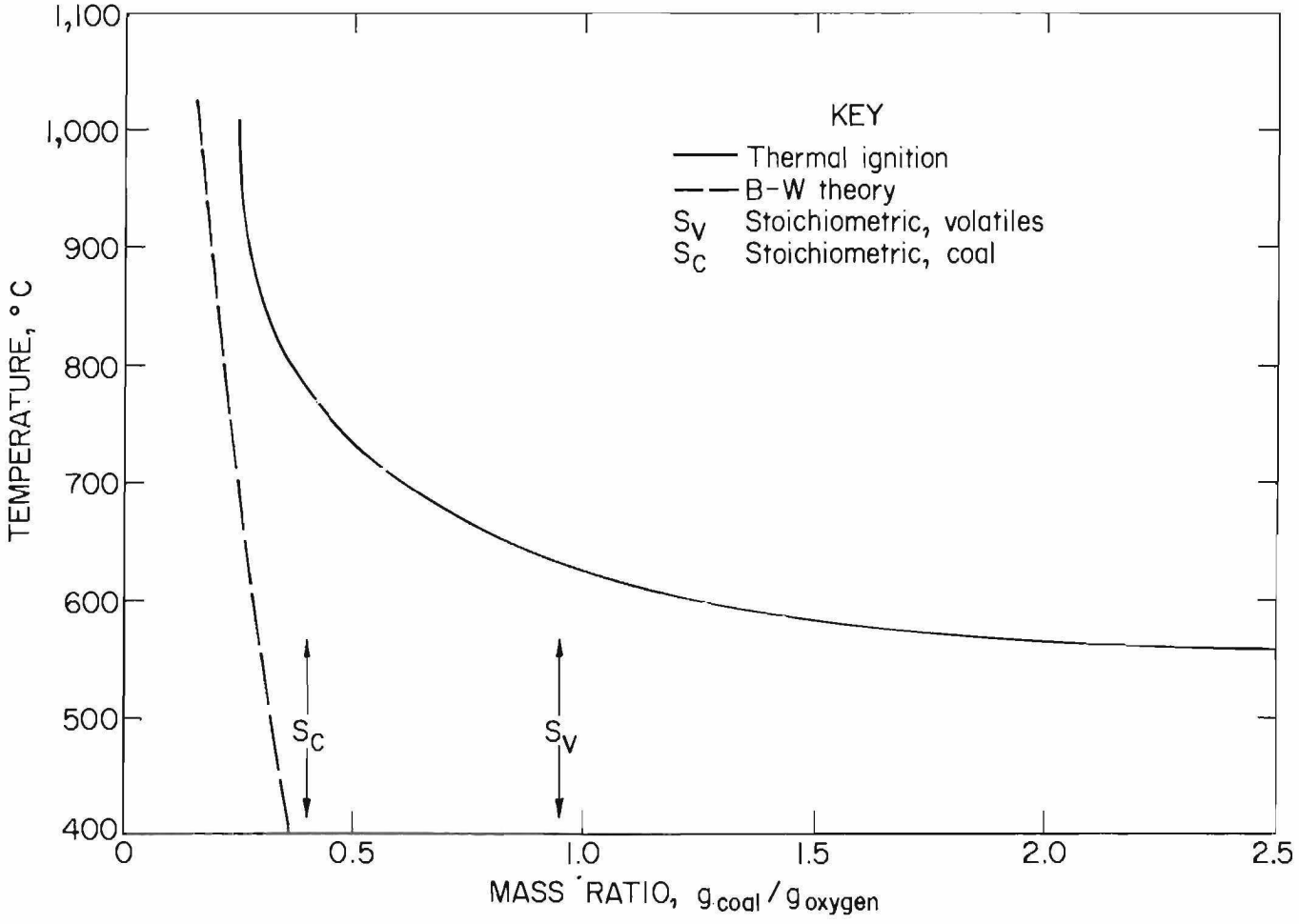

FIGURE 25. - Domain of thermal ignitability as a function of coal-to-oxygen mass ratio for Pittsburgh coal dust with $\bar{D}_s$ _ 55 μm.

limit for the coal (130 g m^{-3}) occurs at a mass ratio that is about 50 pct of stoichiometric with respect to the volatiles. That value is consistent with the values observed for most hydrocarbons in air (32). The minimum AIT in figure 25 occurs at very rich concentrations of combustible volatiles. That result is also consistent with previous ignition studies of heavy hydrocarbon-air mixtures (32).

A summary of all the data obtained for the particle size dependences for both the thermal ignitability data and the lean limit data (15, 17) of Pittsburgh coal is shown in figure 26. The minimum AIT values are summarized in panel A and the lean limit data in panel B. The latter data were obtained in an 8-L chamber at ambient temperatures with an apparatus and method previously described (13, 16). The thermal ignitability and flammability limit curves have similar shapes in that both are intially flat below some threshold or characteristic size. Thus, for Pittsburgh coal, the lean limit and the minimum AIT are both independent of particle size for all sizes below some characteristic diameter. Above that diameter, both curves rise and soon show a marked size dependence. Eventually, they reach a critical diameter above which the dust cloud is nonexplosive at any concentration or entirely nonignitable at any reasonable temperature.

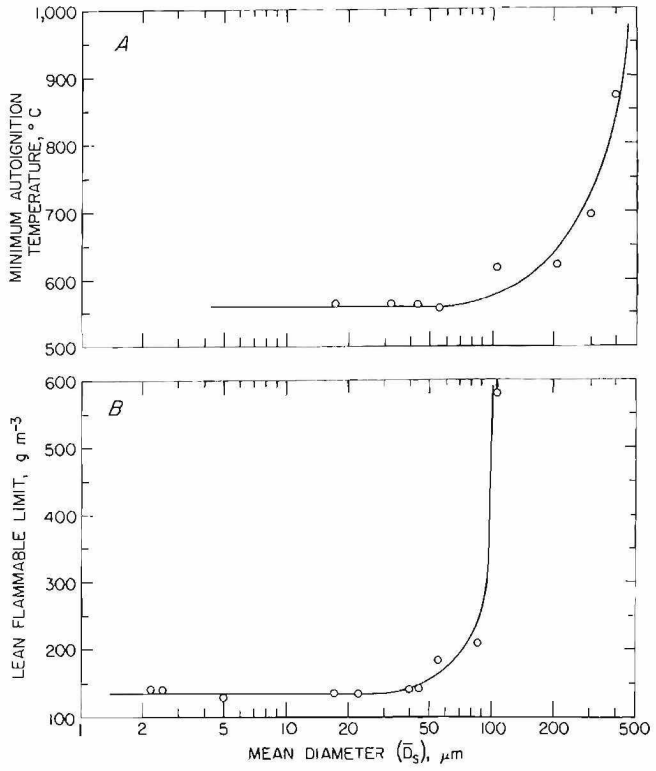

FIGURE 26. - Minimum autoignition temperature and lean flammable limit as a function of particle size for Pittsburgh coal dust. *A*, 1.2-L furnace thermal ignition; *B*, 8-L chamber at 25° C using chemical match ignitor.

A quantitative model for this behavior has been presented elsewhere (15, 17). For the finer particles, the limit concentration and the minimum AIT are size invariant because the devolatilization rate of the particles is so rapid that the overall combustion process is controlled by chemical reaction and diffusion rate processes in the gas-phase mixture of volatiles in air. At the larger particle sizes, the rate of devolatilization appears to limit the overall rate of flame propagation through the mixture. Therefore, for the coarser particles, the mass concentration of dust required to generate a limit concentration of combustible volatiles increases markedly, and a particle size dependence appears. For the lean limit at room temperature this shift in rate control occurs at a characteristic diameter of about 50 μm for Pittsburgh coal. Because of the relatively short preheating time available in the combustion wave, the devolatilization rate decreases rapidly as the particle size increases, and the required dust concentration rises steeply (fig. 26). For the thermal ignitability in the 1.2-L furnace, the shift in rate control as the particle size increases is more gradual because of preheating before ignition, which increases the initial enthalpy and enhances the devolatilization rate. Furnace preheating thus decreases the subsequent steepness of the curve. For the lean limit at 25° C, the critical size is reached rapidly as the diameter doubles (from 50 to 100 μm). For the AIT value in the heated furnace, the critical size is approached more slowly as the diameter quadruples (from 100 to 400 μm).

POCAHONTAS SEAM BITUMINOUS COAL

The thermal ignitability data for four sizes of Pocahontas coal dust are shown in figure 27. The flammability and thermal ignitability domains for this lower volatility (16 pct) coal are similarly delineated. The minimum AIT is 550° C for the finest size studied, and there is a measurable particle size dependence throughout the size range

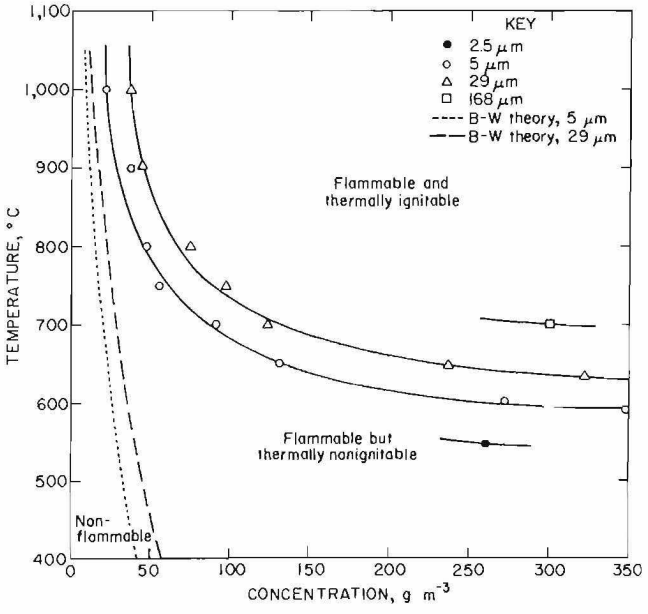

FIGURE 27. - Domain of thermal ignitability for several narrow size distributions of Pocahontas coal dust.

shown. The B-W theory lines are shown for two sizes of dust. The theoretical lines are extrapolated from the room temperature lean limit values measured in the 8-L chamber (15).

The minimum AIT for a broad distribution of Pocahontas coal (with 100 pct minus 120 mesh, 90 pct minus 200 mesh, $\bar{D}_s$ = 12 μm, and $\bar{D}_w$ = 28 μm) is 625° C. For a similar broad distribution of the higher volatility Pittsburgh coal dust, the minimum AIT is 560° C.

A summary of the particle size dependence data for Pocahontas coal dust is shown in figure 28. The measured thermal ignitability in air is shown in figure 28A, and the lean limit in air obtained in the 8-L chamber at room temperature (15) is shown in figure 28B. Both are plotted versus the surface mean diameter. The characteristic diameter at which a particle size dependence first appears for the lean limit data is about 15 μm, much smaller than for the higher volatility Pittsburgh coal. The shift is even more marked for the thermal ignitability curve, which has an upward slope even at diameters as low as 2 μm. The data for narrow size distributions show that the lowest lean limit, observed at fine sizes below 10 μm, is comparable to that measured for Pittsburgh coal. This observation is interpreted to mean that at flame heating rates, the real volatilities for the finer sizes of the Pocahontas coal are comparable to those of Pittsburgh coal. The thermal ignitability behavior for the Pocahontas coal shows a similar trend, and although its AIT is significantly higher than the Pittsburgh coal values for most sizes of interest, the finest size Pocahontas coal has a minimum AIT value that is essentially equal to the lowest Pittsburgh value.

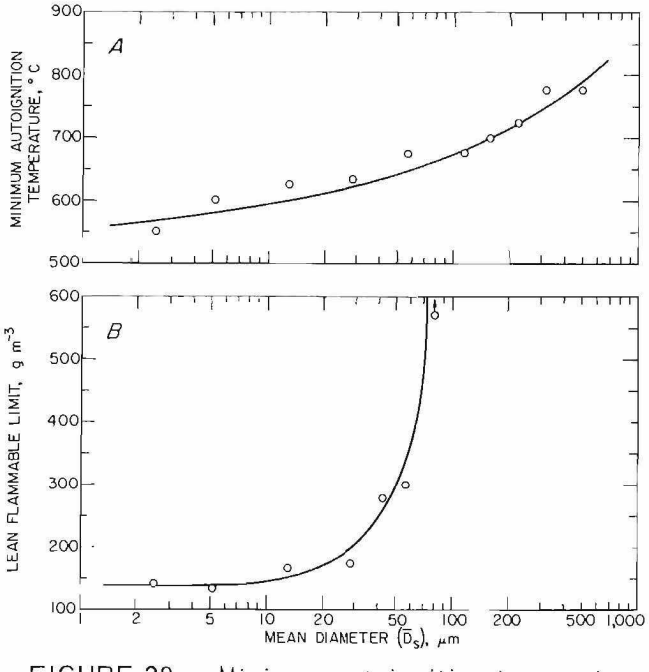

FIGURE 28. - Minimum cutoignition temperature and lean flammable limit cs a function of particle size for Pocahontas coal dust. *A*, 1.2-L furnace thermal ignition; *B*, 8-L chamber at 25° C using chemical match ignitor.

The more marked particle size dependence for the nominally lower volatility Pocahontas coal is consistent with data previously reported for the strong O_2 dependence of the lean limit (13). Both the higher sensitivity to particle size shown here and the strong O_2 dependence described earlier are parallel reflections of a similar property; Pocahontas coal appears to have a greater variability in its real volatility and in its rate of devolatilization as a function of heating rate.

A comparison of the minimum AIT curves of figures 26 and 28 show that the furnace preheating effect is even more pronounced for Pocahontas coal than for Pittsburgh coal. In fact, the two thermal ignitability curves cross at a particle size of 320 μm, where both coals have the same AIT of 750° C. For the coarser dusts (above 320 μm), the Pocahontas coal can be ignited at a lower temperature than the Pittsburgh coal. Preheating the Pocahontas coal before ignition thus increases its relative rate of devolatilization to the point that it eventually becomes more ignitable than Pittsburgh coal at very coarse sizes. A similar crossing of flammability curves for the two coals was observed for their lean limits at elevated O_2 levels (13).

SUBBITUMINOUS COAL

The thermal ignitability data for a subbituminous coal (a powerplant blend of several western subbituminous coals) with an average moisture content of about 10 pct is shown in figure 29. The minimum AIT for the as-received coal was 475° C. The dried coal had a minimum AIT of 455° C. The subbituminous coal is therefore substantially more ignitable than the bituminous coals in either the as-received or the dried state. In the latter case, its minimum AIT is some 100° C below that of Pittsburgh bituminous coal.

LIGNITE

The thermal ignitability data for a North Dakota lignite with a moisture content of about 25 pct is shown in figure 30. The minimum AIT for the as-received lignite was 600° C. That value dropped significantly to 550° C when the lignite was dried. The ignitability of dried lignite is comparable to that of Pittsburgh coal.

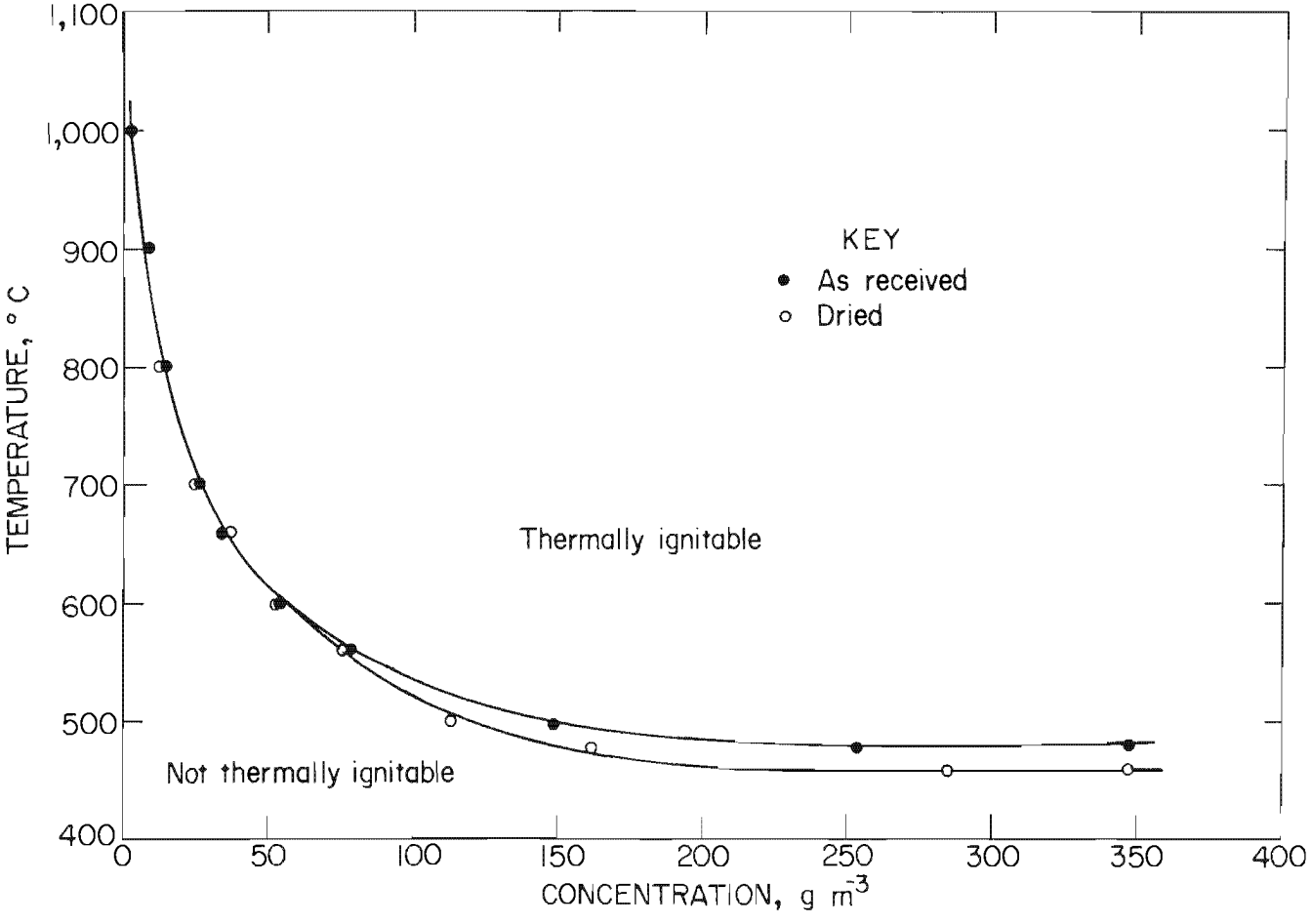

FIGURE 29. - Thermal ignitability data for a subbituminous coal dust, as received and dried.

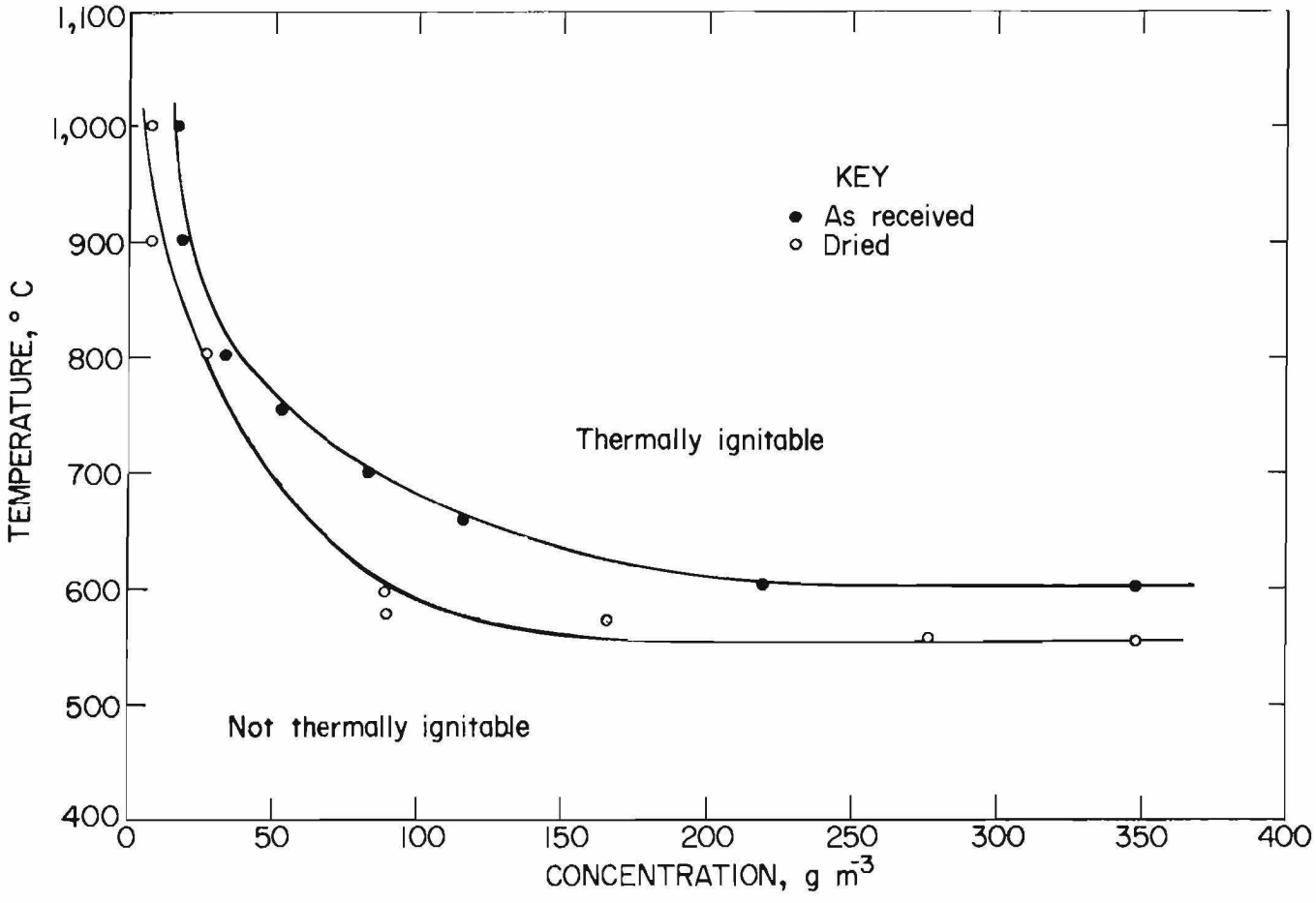

FIGURE 30. - Thermal ignitability data for a lignite dust, as received and dried.

ANTHRACITE

The minimum autoignition temperature for an anthracite dust with 6.6 pct volatility and a very fine particle size ($\bar{D}_s$ = 5 μm) was 780° C in the 1.2-L furnace. This value was only reached at very high concentrations, near 1,100 g m^{-3}. By comparison, previous researchers (25) measured a minimum AIT of 730° C for 8.2-pct-volatile anthracite and 840° C for 4.0-pct-volatile anthracite in the Godbert-Greenwald furnace.

OIL SHALE

Data were also obtained for three oil shale dusts of varying kerogen contents. The measurements are shown in figure 31 for shale dusts whose Fischer assays (31) showed oil contents of 0.10, 0.15, and 0.23 L/kg (25, 35, and 55 gal/ton). The minimum AIT values for all three dusts were the same, 475° C. However, that minimum was reached at much higher dust concentrations for the shales with lower oil contents. Additional data on the fire and explosion hazards of oil shale are found in reference 30.

POLYETHYLENE

The data for polyethylene dust, a completely volatilizable, saturated, hydrocarbon solid of very high initial molecular weight, are shown in figure 32.

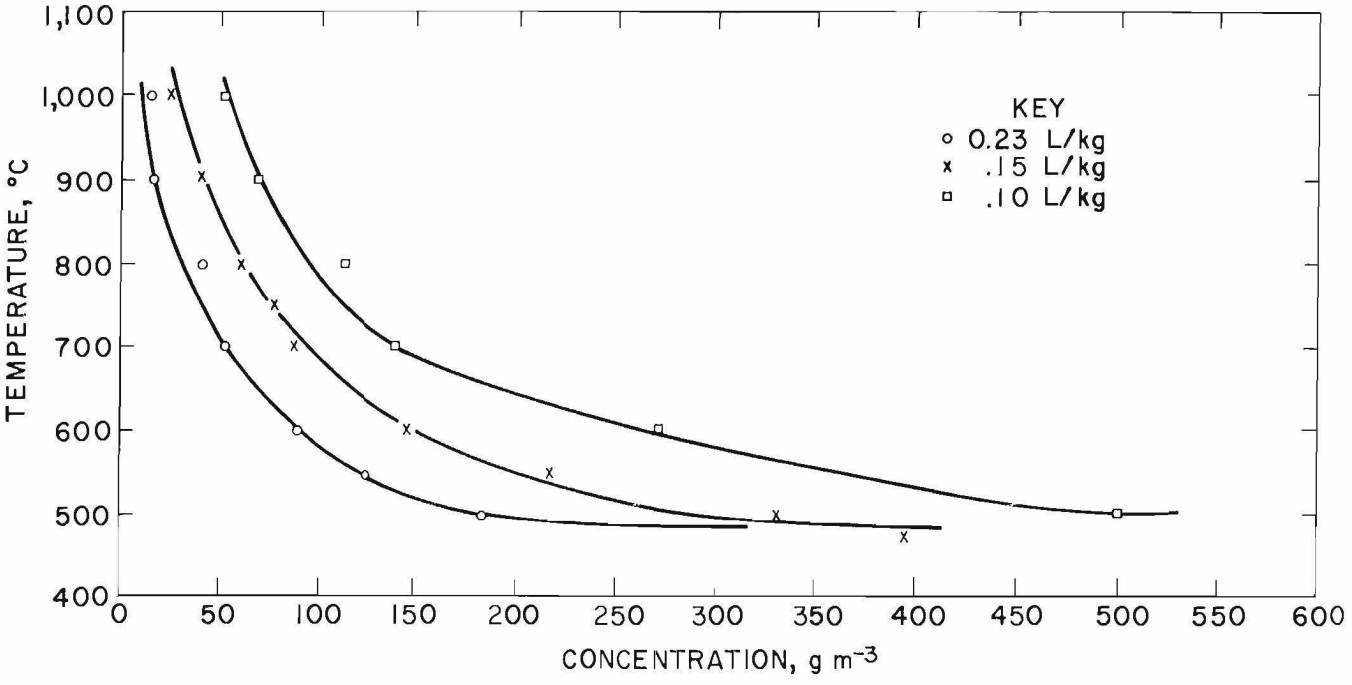

FIGURE 31. - Thermal ignitability data for three grades of oil shale.

Unlike the coals, polyethylene contains no aromatic structures and no oxygen, sulfur, nitrogen, or inorganic ash. Accordingly, it is completely volatilizable at relatively low temperatures and leaves no carbonaceous char residue under normal pyrolysis or combustion. Its minimum AIT is 400° C, and that value is reached at the lower concentration of 130 g m^{-3} (compared to about 250 g m^{-3} for Pittsburgh coal) because of its much higher volatility than the coal. Its domain of flammability is delineated using the B-W theory starting with polyethylene's measured room temperature lean limit (13) of 45 g m^{-3}. Again there is a broad region of temperatures below 400° C but to the right of the B-W theory curve where the dust is flammable but not thermally ignitable.

It is again instructive to try (as in fig. 25) to account for the diminishing oxygen content at the elevated temperatures and therefore lower gas densities involved in these ignitability experiments. This is again done by transforming the mass concentration scale in figure 32 to a mass ratio scale. The transformed flammability and ignitability curves are so plotted in figure 33, where the independent variable is now the mass ratio of polyethylene to oxygen in the 1.2-L furnace. Since polyethylene is completely volatilizable, the complication involved in distinguishing between the volatiles and the char and ash residue for coal in figure 25 is no longer necessary. A stoichiometric ratio of polyethlene to oxygen corresponds to a mass ratio of 0.29, and that value is

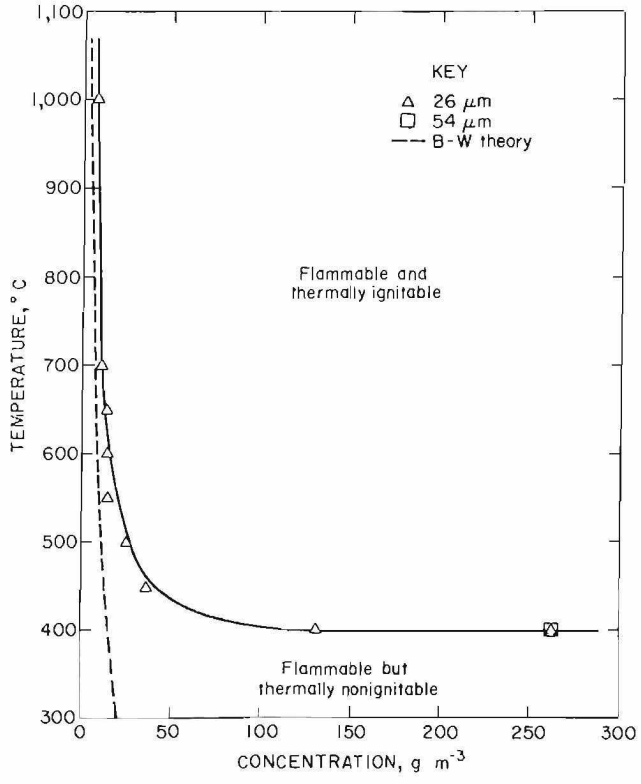

FIGURE 32. - Thermal ignitability data for two sizes of polyethylene dust with $\bar{D}_s$ 26 and 54 μm.

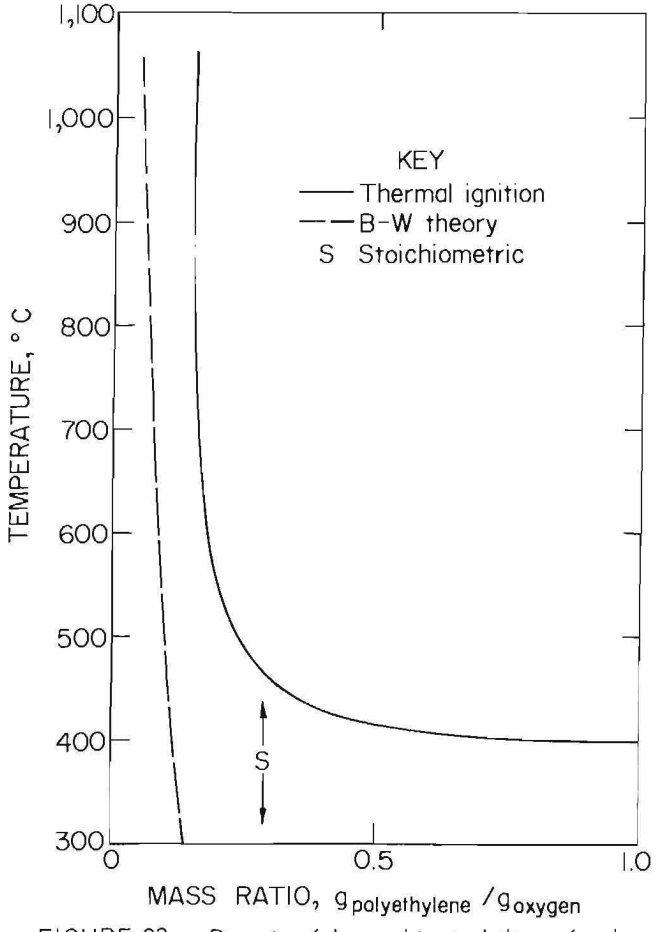

FIGURE 33. - Domain of thermal ignitability of polyethylene dust as a function of fuel-to-oxygen mass ratio.

plotted as a vertical line in figure 33. As was the case with the coals, the minimum AIT occurs at a relatively rich concentration of fuel to oxygen. That result suggests that the polyethylene pyrolysis products that participate in the thermal ignition process are relatively high-molecular-weight hydrocarbons. At the higher temperatures, the data do not approach the B-W theory curve more closely because the lowest mass concentration of dust that could be accurately weighed and dispersed was about 10 g m^{-3}.

A summary of the particle size dependences observed for both the lean limit obtained in the 8-L chamber (15) and the minimum AIT of polyethylene powder is shown in figure 34. Polyethylene's lowest lean limit in panel B is about 45 to 50 g m^{-3}, and its minimum AIT in panel A is 400° C. Similar to the bituminous coal data (figs. 26 and 28), both curves are initially flat at the finer sizes until a characteristic size is reached at which point the curves turn upward. Because of its higher volatility and its greater rate of devolatilization, a particle size dependence for the lean limit first appears at a diameter of 100 μm, which is much larger than the 50 μm found for Pittsburgh coal dust. For the same reasons, the preheating effect in the thermal ignitability curve is more pronounced. The AIT curve increases very slowly above 150 μm, and the critical size (above which the dust will not ignite) is not even approached at diameters as large as 500 μm. On the other hand, at ambient temperatures, the critical size for the lean limit is reached quite rapidly as the diameter increases from 100 to 150 μm.

In measuring the thermal ignitability domain for the larger polyethylene dusts,

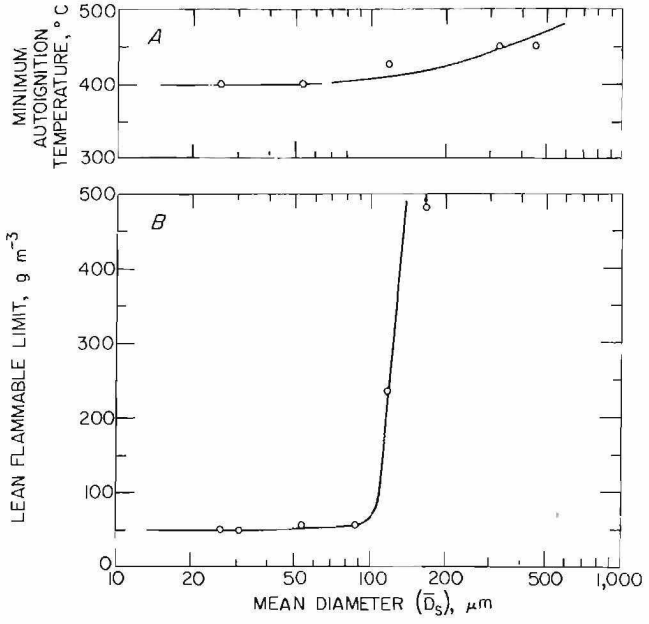

FIGURE 34. - Minimum autoignition temperature and lean flammable limit as a function of particle size for polyethylene dust. *A*, 1.2-L furnace thermal ignition; *B*, 8-L chamber at 25° C using chemical match ignitor.

an interesting effect was observed. This is shown in the temperature versus concentration plot for 330-μm polyethylene in figure 35. The lower temperature portion of the ignitability curve is relatively normal, corresponding to the 450° C minimum AIT value on figure 34. At elevated temperatures between 450° and 550° C, the curve continues to behave normally; however, above 550° C an anomaly is observed. The curve bends back on itself and becomes double valued; that is, the system appears to become less ignitable at the more elevated temperatures. Above 725° C, no ignitions were observed even at very high dust concentrations.

This anomalous, double-valued behavior is observed only for the coarser dusts above 300 μm. One hypothesis is that it occurs because the rate of devolatilization for these large particles is so slow that volatiles are oxidized heterogeneously at the surface of the furnace before an explosive concentration can be generated in the gas phase. If so, it is

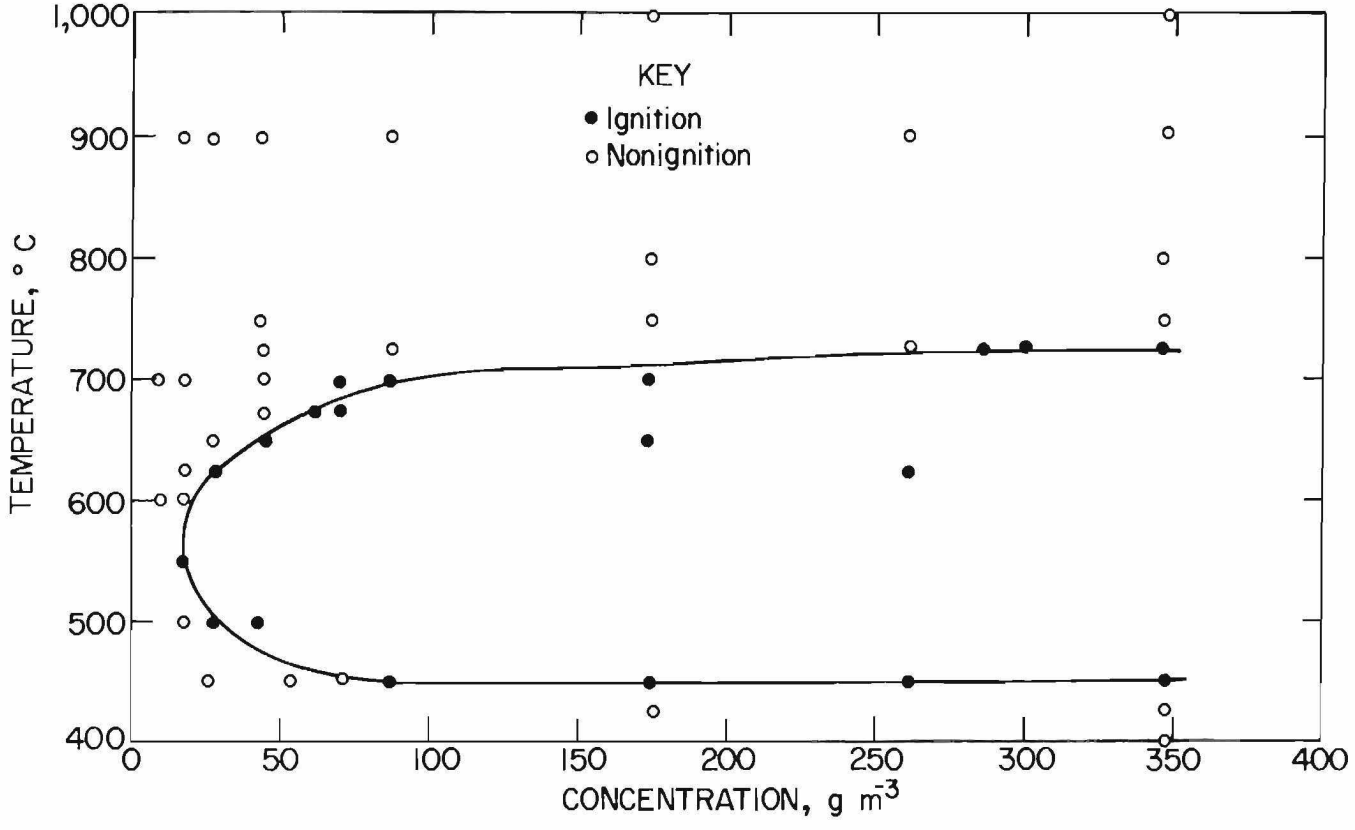

FIGURE 35. - Thermal ignitability data for 330-μm polyethylene dust.

expected that this anomalous behavior should be sensitive to the surface-to-volume ratio of the system, i.e., to the size of the vessel (22). Gas-sampling data were obtained with the rapid-sampling system in an attempt to resolve this question. The results showed that the amount of oxygen consumed during the tests was similar on each side of the upper boundary of figure 35. Because there were no explosions above the boundary, the oxygen was most likely consumed by much slower, heterogeneous reactions. These data tend to confirm the argument that the anomalous double-valued behavior in figure 35 is indeed caused by a slower competing oxidation process which consumes volatiles and oxygen before a more rapid gas-phase ignition can occur.

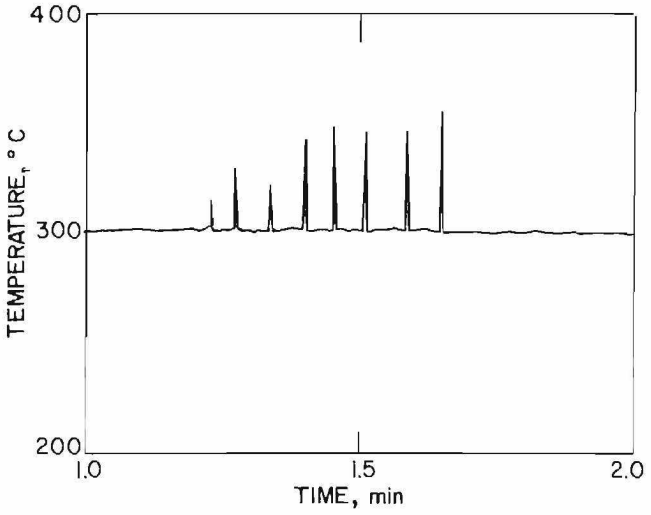

FIGURE 36. Thermocouple trace of the oscillatory flame exhibited by the hydrocarbon decane, $C_{10}H_{22}$.

DECANE

Experiments were also conducted with a pure liquid hydrocarbon. A fixed mass of n-decane ($C_{10}H_{22}$), approximately 510 mg, was placed in a ceramic cup, inserted into the furnace, and allowed to evaporate into the closed system at various temperatures. Although ignition and explosion were not obtained under these circumstances at any initial temperature, the thermocouple traces showed some interesting behavior. The thermocouple trace for an initial oven temperature of 300° C is shown in figure 36. It shows a very distinct, oscillatory cool flame propagation. The oscillation has a period of about 4 sec, and the maximum temperature rise is no more than about 50° C above the initial furnace temperature. Such oscillatory cool flame behavior is characteristic of rich mixtures of heavy hydrocarbons in air (12). Clearly, the pressure rise is not sufficient to rupture the diaphragm, and hence, according to the criterion used here, this does not constitute an ignition.

However, it was possible to obtain normal ignitions if the decane was dispersed into the furnace by an air blast from the dispersion receptacle. In that case the liquid was probably atomized, volatilized, and mixed with the air at a faster rate than was possible when it was contained in a cup. For the dispersed decane, the minimum AIT was 275° C, and that value was reached at a fuel concentration of 90 g m^{-3}. It is interesting to compare that value with those reported using the traditional AIT method for liquids (33). In the traditional method, the liquid is pipetted into an open flask (0.2- to 1.0-L), and the propagation criterion is the visual observation of flame. The value obtained for decane using that method is 208° C. The higher value of 275° C obtained in the 1.2-L furnace is probably related to the more stringent propagation criterion used here. The requirement of both a 0.1- to 0.3-atm overpressure to rupture the diaphragm and visual flame emerging from the furnace is a more severe criterion than visual observation of flame or luminosity somewhere within the open flask.

EFFICIENCY OF INHIBITORS ADDED TO PITTSBURGH BITUMINOUS COAL DUST AT ELEVATED TEMPERATURES

The Godbert-Greenwald and 1.2-L furnaces can also be used for evaluating the effectiveness of various powdered inhibitors. In some earlier experiments (23) before the 1.2-L furnace was built, the Godbert-Greenwald furnace was used to evaluate five fluidized fire extinguisher powders and compare them to limestone rock dust. In these experiments, the Pittsburgh coal dust mass was fixed at 100 mg, the most flammable amount for that experimental procedure, as shown in figure 18. Various amounts of inhibitor were added to the coal dust, and the furnace ignition temperatures were measured for the various mixtures. The data are shown in figure 37. The incombustible content shown at the top of figure 37 includes the inhibitor content plus the 8 pct ash and moisture in the coal. The five fluidized powders' names and chemical symbols were BCD (NaCl), Super K (KCl), ABC ($NH_4H_2PO_4$), BCS ($NaHCO_3$), and Purple K ($KHCO_3$). The other inhibitor was limestone rock dust ($CaCO_3$). The inhibitors fell into two groupings; the NaCl, KCl, and $NH_4H_2PO_4$ almost completely inerted the coal dust at

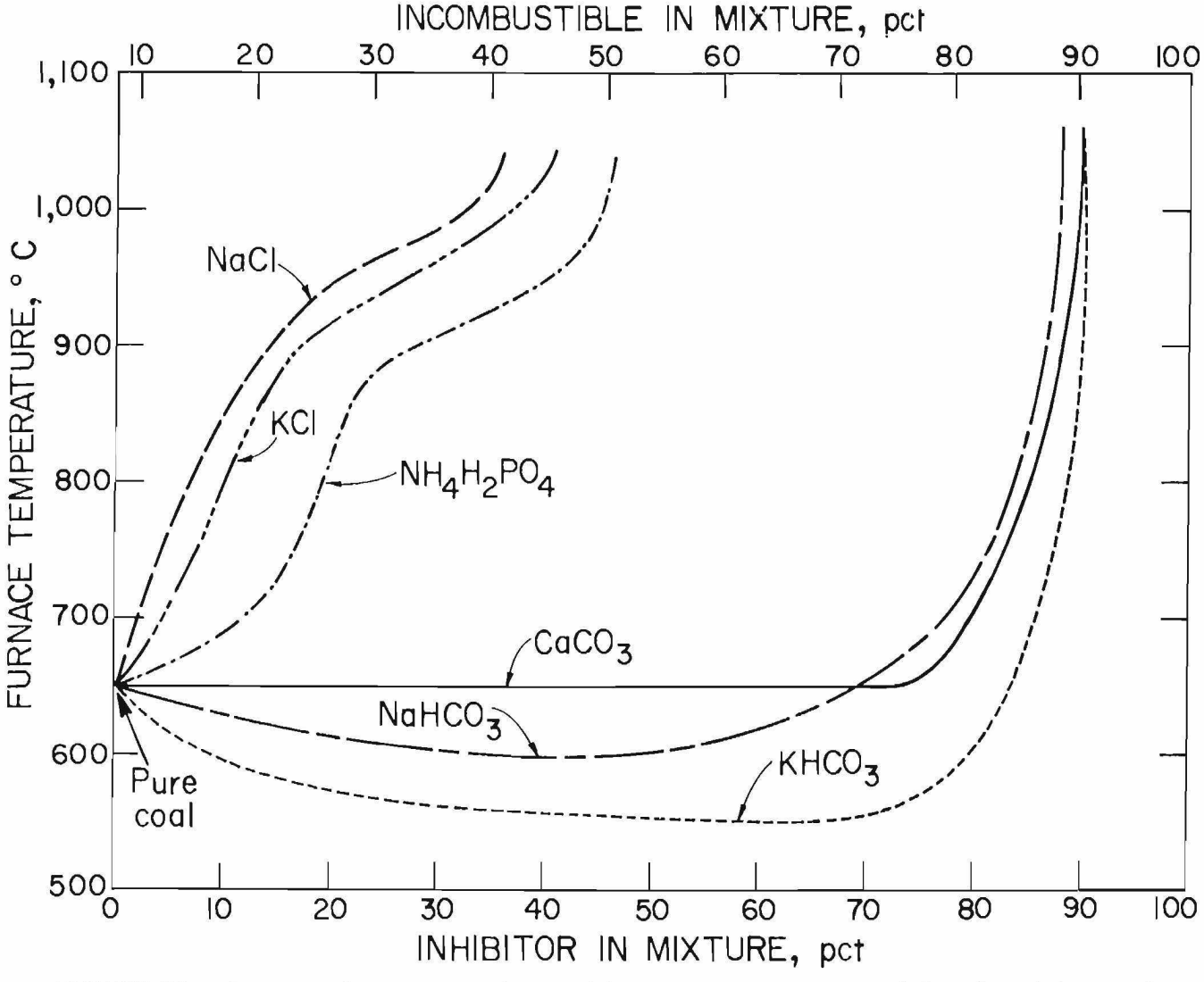

FIGURE 37. - Amounts of various powdered inhibitors necessary to inert 0.1 g of coal dust in the Godbert-Greenwald furnace.

inhibitor contents of about 35 to 45 pct, which raised the ignition temperature to above 1,000° C. The less effective powders, $CaCO_3$, $NaHCO_3$, and $KHCO_3$, required inhibitor contents of about 90 pct to raise the ignition temperature to above 1,000° C.

These results agree partially with full-scale mine tests (13-14, 23) on the amount of inhibitor necessary to quench a coal dust explosion. However, in the mine tests the $NH_4H_2PO_4$ was significantly better than the NaCl or KCl. Experiments in an 8-L laboratory chamber (13-14) at room temperature gave data on the amount of inhibitor necessary to inert coal dust that agree even better with the mine results. Accordingly, the 8-L chamber was used for preliminary testing prior to the more costly full-scale mine tests. The data in figure 37 show that the Godbert-Greenwald furnace also has some value as a screening test for inhibitor effectiveness.

Additional data on the effect of added inhibitors on Pittsburgh coal dust were obtained in the 1.2-L furnace and are shown in figures 38 and 39. The data are for two fluidized fire extinguisher powders: ABC ($NH_4H_2PO_4$) and Purple K ($KHCO_3$). The dust concentration on the horizontal axis is the total dust concentration, including both the coal and the inhibitor. For the ABC powder in figure 38, 80 pct inhibitor almost inerts the coal inhibitor mixture as the ignition temperature is raised to above 900° C. For the Purple K in figure 39, even 80 pct inhibitor has only a small effect on the ignition temperature at high dust concentrations.

In the room temperature tests in the 8-L chamber and the experimental mine, approximately 20 to 25 pct ABC powder is required to totally inert a coal-inhibitor mixture (13-14, 23). In those same experiments 70 to 80 pct Purple K was required to inert a coal-inhibitor

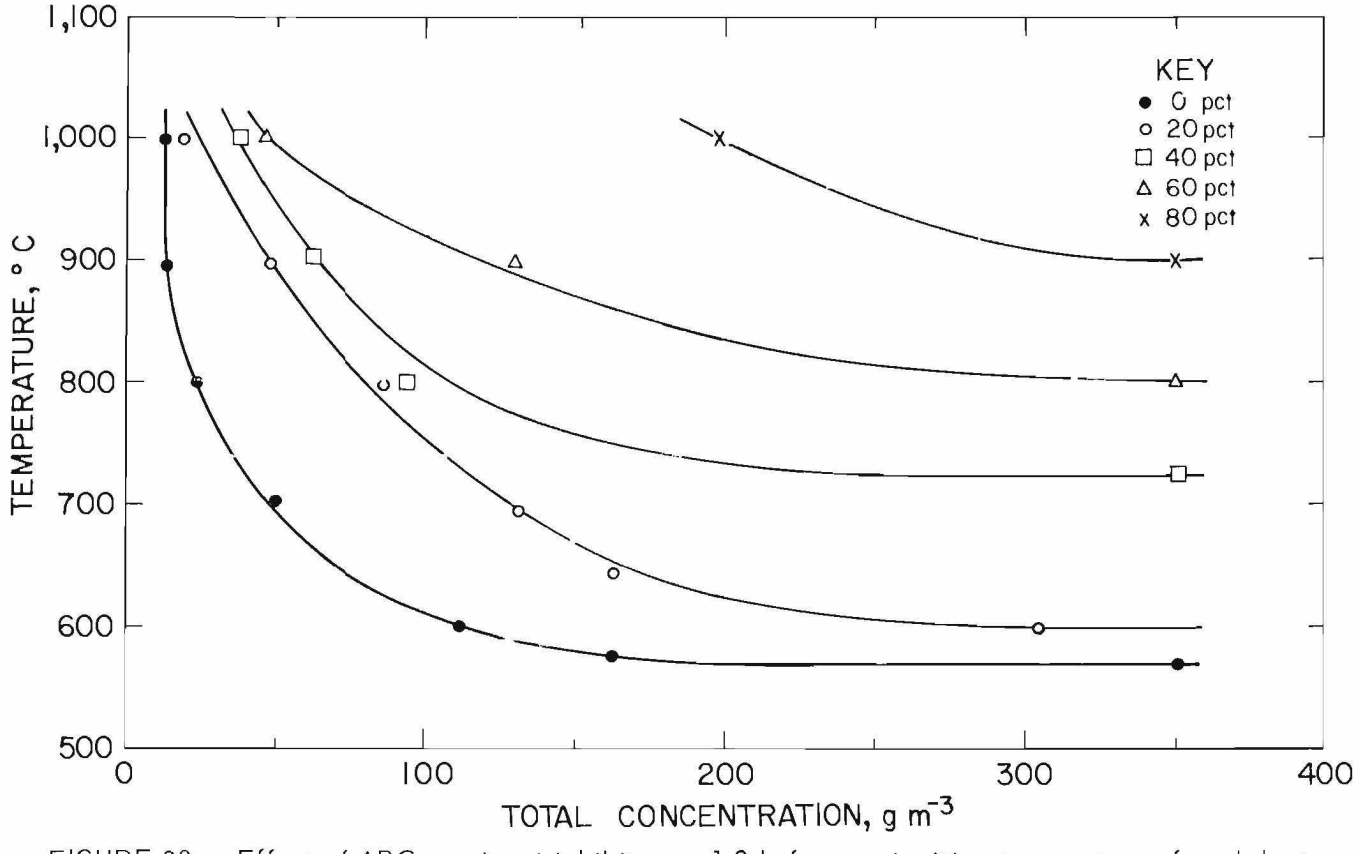

FIGURE 38. - Effect of ABC powdered inhibitor on 1.2-L furnace ignition temperature of coal dust.

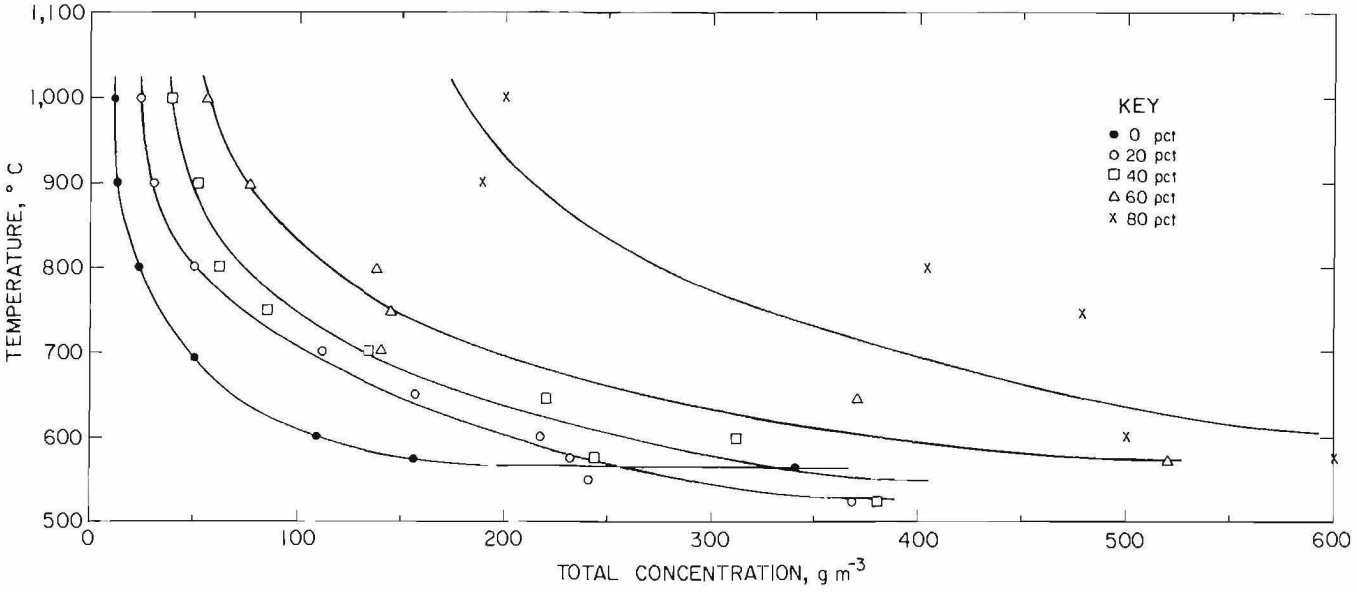

FIGURE 39. - Effect of Purple K powdered inhibitor on 1.2-L furnace ignition temperature of coal dust.

mixture. The data on the poor effectiveness of Purple K as an inhibitor at the higher temperature in the furnaces (figs. 37 and 39) are similar to those at room temperature. ABC, however, appears to be somewhat less effective as an inhibitor when tested at the high furnace temperatures compared to the room temperature data. That is to be expected since flammability increases with increasing initial temperature.

SAMPLING DATA FROM THE 1.2-L FURNACE

A need for analyses of combustion products led to the development of the rapid dust- and gas-sampling device (7) described in the "Apparatus and Experimental Methods" section and shown as part of the 1.2-L furnace in figure 15. The system allows for rapid grab sampling of heterogeneous mixtures of gases and dusts during the preignition and postignition phases of dust explosions.

Figure 40 shows the thermocouple trace as a function of time from an ignition of a coal dust cloud for which gas and dust samples were collected. The thermocouple trace shows a slight drop in temperature as the coal dust and air enter the furnace. The temperature again reaches the set point of the furnace at a later time as the dust heats up during the preignition interval. The rapid increase in temperature at 0.9 sec indicates ignition, with rupture of the diaphragm and flame ejecting outwards. The dust used was Pittsburgh seam bituminous coal with a surface mean particle size of 55 μm and at a concentration of 260 g m^{-3}.

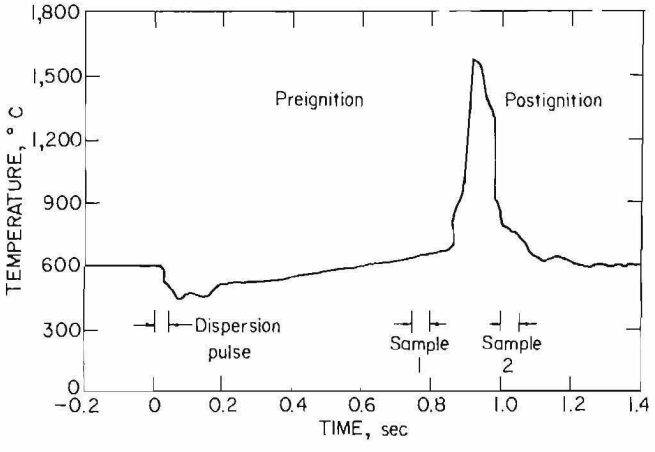

FIGURE 40. - Thermocouple trace for a coal dust explosion showing the preignition and postignition times at which gas and dust samples were obtained using the rapid-sampling system.

In this run, the microprocessor was set to obtain two samples, sample 1 before thermal autoignition (preignition) and sample 2 after ignition and explosion of the dust cloud (postignition).

The gas analyses obtained from two coal dust-air runs at the same initial conditions (260 g m^{-3} and 600° C) are shown in table 2. The sampling time for each run was 50 msec. The analyses were done by gas chromatography. There are a substantial decrease in the O_2 level and an increase in the CO_2 level in the postignition column for both runs. Hydrocarbons (C_1 to C_4) were generated during the preignition or pyrolysis phase and then consumed during the explosion that occurred after ignition. Hydrogen was less than 0.1 pct for all analyses; the remainder was N_2. The explosions resulted in a 40-pct reduction in the O_2 levels, consumption of the hydrocarbons, and a corresponding increase in the CO_2 levels. Because the diaphragm ruptured before the flame filled the entire chamber, not all the oxygen was consumed.

The coal dust particles were also sampled during the two experiments. The results of their scanning electron microscope (SEM) analyses (28) are presented at two magnifications in figure 41. The unburned dust is on the left (panels A-B), the preheated dust is in the center (panels C-E), and the postignition dust is on the right (panels F-H). Notice that the unburned dust has sharp edges. The preheated dust is that which has been dispersed into the furnace and heated to 600° C but has not yet ignited. There is clearly substantial devolatilization occurring even during preignition with the unburned but preheated dust samples containing many blowholes. That observation is consistent with the plentiful hydrocarbon production seen in the preignition data shown in table 2. The postignition samples correspond to the dust residues after the explosion. The postignition dust samples are also strongly devolatilized, as expected.

TABLE 2. - Gas analyses of a coal dust explosion, obtained using the rapid-sampling system, percent

Gases	Preignition		Postignition	
	Run 1	Run 2	Run 1	Run 2
O_2.....	19.3	19.5	12.6	12.0
CO_2.....	.4	.3	6.1	5.7
CO.....	.6	.7	.2	1.3
HC, C_1 to C_4..	1.06	.62	.07	.10

ELECTRICAL SPARK IGNITABILITY IN THE 1.2-L FURNACE

The relationship between the flammability limit and the thermal ignitability limit for Pittsburgh coal dust in air was depicted in figure 20. Two curves were depicted; the lower one delineated the region of flammability, and the upper one delineated the region of thermal ignitability. As noted before, the flammability limit is the boundary at which a dust cloud is capable of propagating a flame after ignition by a sufficiently strong external energy source inserted into the cloud. The thermal ignitability limit is the boundary at which a dust cloud will autoignite without the addition of any external energy. Alternatively, the flammability limit can be described as the boundary where the dust cloud is ignited by an external, local ignition source with an energy approaching infinity so that its ignition probability is unity. The thermal ignitability curve can be described as the boundary where the external ignition energy required is zero and the cloud autoignites owing to its own intrinsic reactivity at that temperature. Although mixtures are flammable in the region between the two curves, they are not thermally autoignitable. However, if other ignition sources are present in the system in that intermediate region, then the explosion probability becomes equal to the ignition probability.

One type of ignition source that is of interest and that can have a marked effect on the ignitability of the system is an electric spark source. There have been several studies (2, 10, 21, 24) of

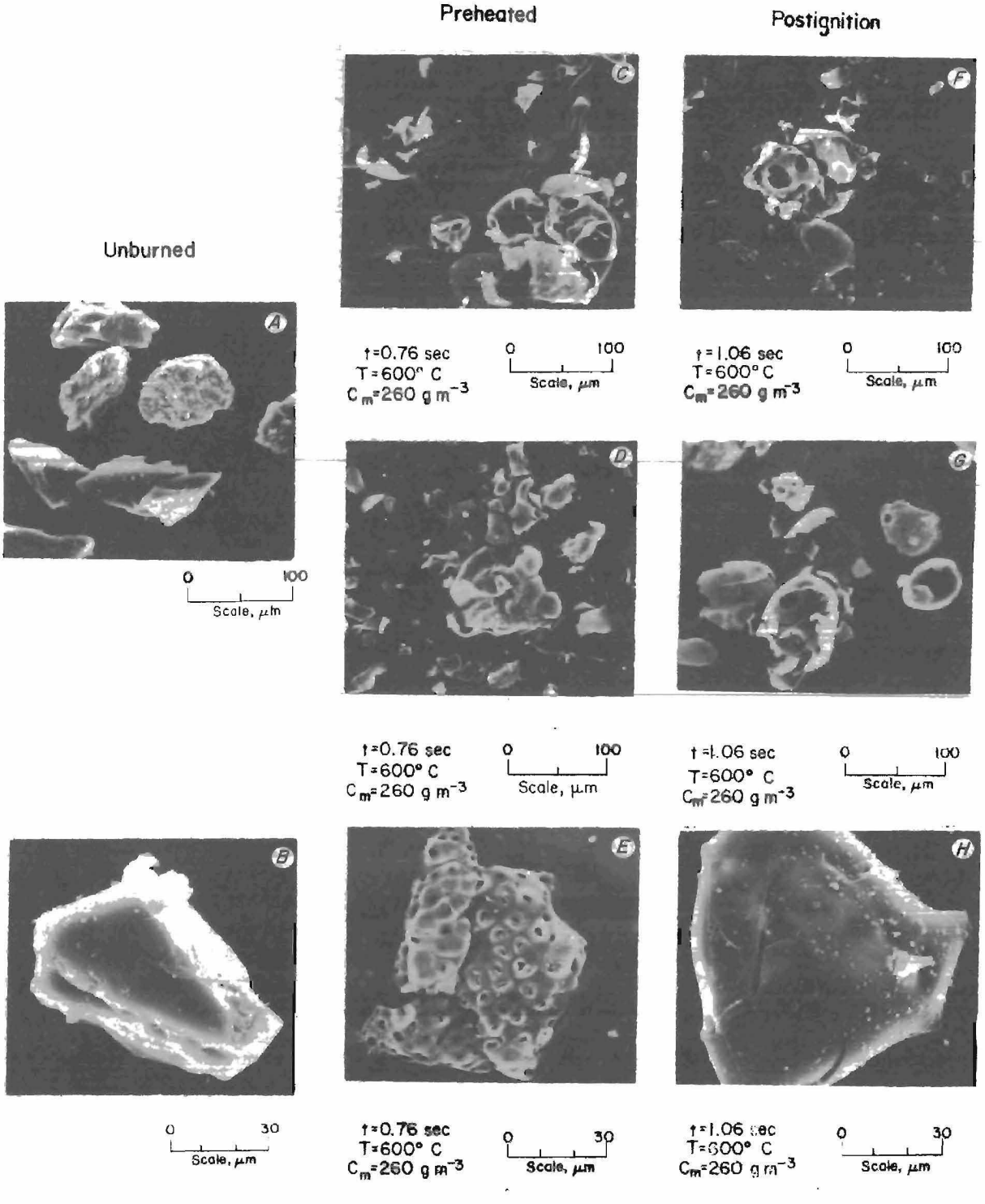

FIGURE 41. - Scanning electron microscope photographs of 55-μm Pittsburgh coal dust sampled from 1.2-L furnace. The preignition and postignition dusts are compared to the unburned dust.

the geometrical and electrical characteristics associated with spark ignitions of gases, vapors, and dusts.

The 1.2-L furnace has also been used to study the electrical spark ignition of preheated coal dust clouds. The spark energy requirements for ignition of coal dust clouds were measured as a function of concentration and temperature. A schematic of the system used to determine the spark efficiency is shown in figure 42. The electrical energy for the spark is obtained by charging a capacitor of capacitance (C) to some known potential (E). The spark is generated by discharging this capacitor through one of two high-voltage transformers (rated at 15-kV output for 110- or 277-V ac input) into an electrode gap contained in a small closed volume (V). The stored electrical energy in the capacitor is equal to $1/2\ CE^2$. The energy deposited into the gas is proportional to $V\Delta P$, where ΔP is the measured pressure rise in the fixed volume V. The lower part of figure 41 shows a trace of the pressure pulse resulting from an electrical spark in a closed volume. Spark efficiency is proportional to the $V\Delta P$ energy deposited into the gas divided by the electrical energy stored on the capacitor. For purposes of this report let

$$\text{spark efficiency} = \frac{V\Delta P}{1/2\ CE^2} . \qquad (4)$$

The spark efficiencies obtained from such $V\Delta P$ measurements at room temperature in a 147-cm^3 vessel are shown in figure 43 as a function of electrode distance. The experiments were done at a constant large capacitance of 2,880 μF and at an input of E = 300 V dc. The spark efficiency increases with increasing gap distance until an optimum distance is reached. At

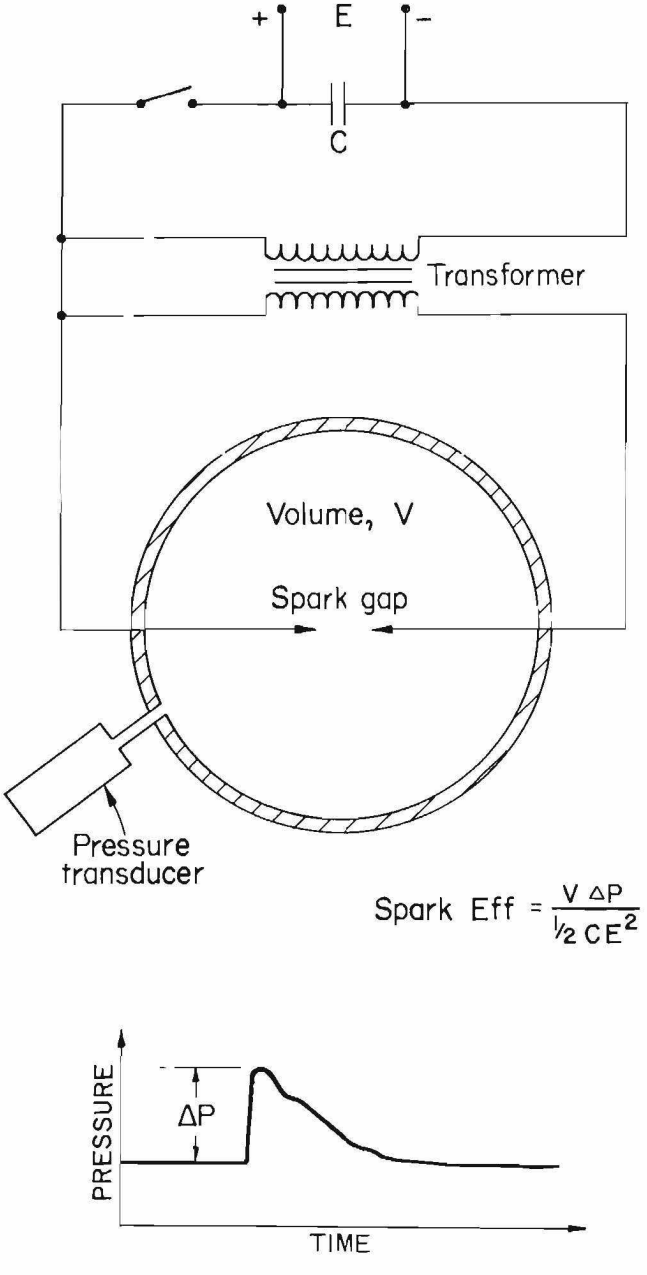

FIGURE 42. - Schematic of the electrical system used to determine spark efficiency.

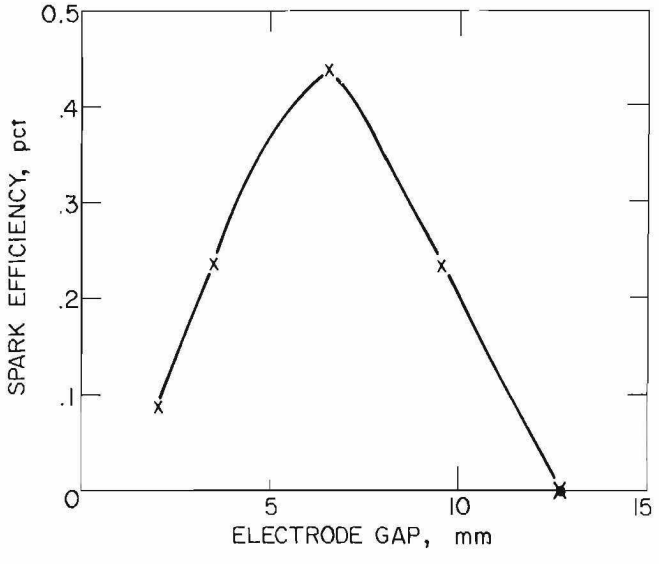

FIGURE 43. - Spark efficiency as a function of electrode gap distance.

greater distances the electric field strength is insufficient for breakdown and the efficiency drops to zero. Note that even the maximum spark efficiency is very low for this very high capacitance value.

The data shown in figure 44 were obtained by keeping the voltage constant at 300 V and varying the capacitance and gap distance. At the lower capacitance values there is a linear relationship between the VΔP energy and the capacitance. However, at the higher capacitance values, there is a leveling off of the deposited energy, especially for the smaller spark gaps. The electrical energy stored on the capacitors is shown on the top scale in figure 44. The spark efficiency (as defined by equation 4) for the 8-mm gap declines from about 12 pct at the low capacitance values to about 5 pct at 300 μF and to values less than 1 pct for the 2,880-μF capacitor data in figure 43.

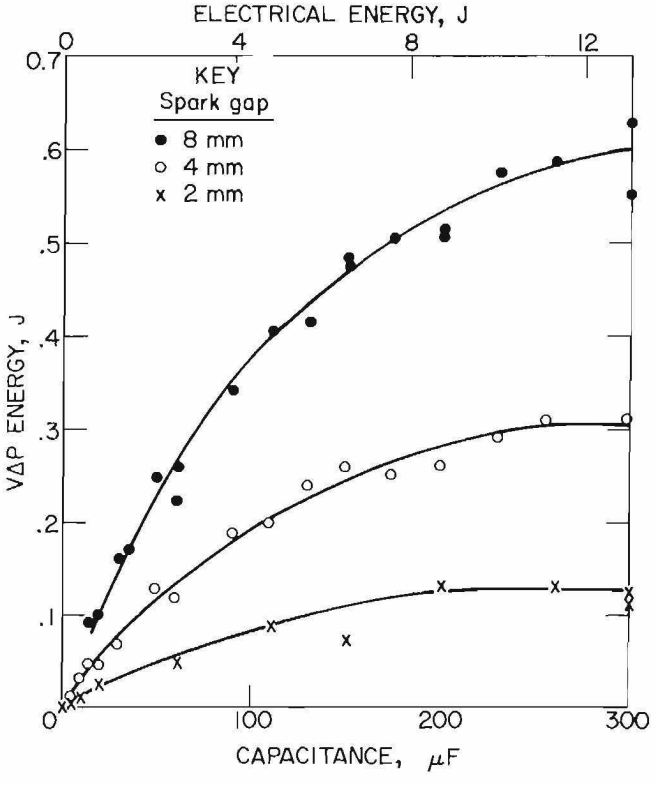

FIGURE 44. - Spark efficiency as a function of capacitance for three electrode gap distances.

The dramatic effects of introducing such an electrical ignition source into the 1.2-L furnace are shown in figure 45 which shows the B-W theory and thermal ignitability curves from figure 20 for Pittsburgh coal dust. The three data curves at the lower right illustrate the combined effect of thermal and spark ignition for Pittsburgh coal dust. For any one of these three energies, the region above and to the right of the curve is both flammable and spark ignitable. If we take, for example, the curve for VΔP = 0.5 J, the area above the curve is flammable and spark ignitable, but the area between this curve and the B-W theory curve is flammable but nonignitable at this spark energy. A very weak spark (VΔP = 0.05 J) shows a significant shift in the data, requiring higher temperatures and concentrations for ignition.

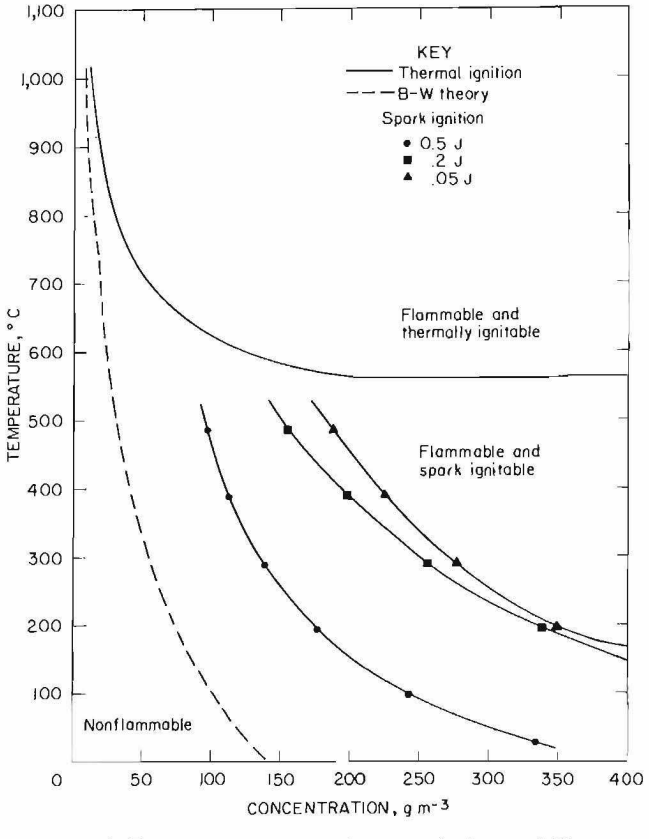

FIGURE 45. - Electrical ignitability of Pittsburgh coal dust for three spark energies as a function of temperature and dust concentration.

CONCLUSIONS

These experimental investigations have shed considerable light on a variety of important questions. They have improved our understanding of the kinetic mechanism by which dust clouds ignite thermally. They provide an important insight into the variables involved in determining the effective electrical ignition energy required to ignite a dust cloud. There are still substantial unresolved issues in those two areas, but those uncertainties should not obscure the central conclusion of this study. That conclusion is that this new 1.2-L furnace (or its equivalent with a larger volume) together with its improved testing procedure should replace the older Godbert-Greenwald furnace.

The new 1.2-L furnace is better than the Godbert-Greenwald furnace because of (1) its larger volume (1.2 versus 0.3 L), (2) the more uniform dust dispersion due to its confined rather than open volume, (3) the longer exposure time of the dust cloud in the high-temperature region, and (4) the more stringent and realistic explosion criterion, which includes both rupture of the diaphragm and flame ejecting from the furnace.

These improvements have led to significantly lower measured minimum autoignition temperatures in the new 1.2-L furnace as compared to those in the Godbert-Greenwald furnace as shown in table 3. The dusts listed in table 3 were the only dusts tested in the present study that could also be accurately identified with dusts listed in references 25 and 27. All of the dusts were 90 to 100 pct minus 200 mesh (74 μm), and all except lycopodium had fairly broad size distributions. The lycopodium had a very narrow size distribution with a mean diameter of 27 μm. It should be noted that very fine size distributions of Pittsburgh or Pocahontas coal give even lower minimum AIT values in the 1.2-L furnace, as shown in figures 26 and 28.

TABLE 3. - Comparison of dust cloud minimum autoignition temperatures in Godbert-Greenwald furnace and new 1.2-L furnace, °C

Dust	Godbert-Greenwald furnace (25, 27)	1.2-L furnace
Bituminous coal:		
Pocahontas Seam....	640	625
Pittsburgh Seam....	610	560
Gilsonite, Utah.....	580	490
Polyethylene.....	450	400
Lycopodium.....	480	435

NOTE.--All of the dusts were 90 to 100 pct minus 200 mesh (74 μm), and all except lycopodium were fairly broad size distributions.

Even the new furnace may not yet represent the optimum size, as was indicated from the double-valued character of the ignition data for very coarse polyethylene dust (fig. 35). Accordingly, the data should be rechecked in larger test volumes with smaller surface-to-volume ratios. Such larger furnace volumes should reduce any competing surface oxidation rates and reduce wall heat losses to the surroundings. It remains to be determined whether larger test volumes would further reduce the minimum AIT's.

In general terms, the flammability or explosivity of a system is describable as some limiting geometric surface in a thermodynamic state-space whose independent variables are the initial temperature (T), the initial pressure (p), and the initial composition variables (x_i's). That surface separates a domain of flame propagation within from a region outside that surface where flame propagation is not normally possible. That mathematical surface, the flammability limit surface, describes a discontinuity in the real combustion behavior of any system. Its exact "size" and "shape" in state-space is of basic significance in evaluating

the practical hazards involved in the use of fuels, refined substances, and synthetic chemicals. From that point of view, figure 20 is, in effect, a temperature versus concentration cross section is such a state-space. It is the state-space of Pittsburgh coal dust mixed with air taken at the constant-pressure plane of 1 atm. The chain-dashed line in figure 20 is the intersection of the flammability limit surface with that constant-pressure plane, and the remaining two variables are the initial temperature and the initial dust concentration. The thermal ignitability data are plotted in that same temperature-concentration plane and generate a new curve, the thermal ignitability curve, which is the solid line. Clearly the thermal ignitability domain is smaller than the flammability domain and is always contained within it.

Two quantities that characterize the domains of flammability and thermal ignitability are defined in figure 20. The one is the lean limit at ambient conditions, which is sometimes referred to as the minimum explosive concentration. The other is the minimum autoignition temperature (AIT), which is approached asymptotically at high dust concentrations and is sometimes called the minimum cloud ignition temperature. The data points in figure 20 show clearly that the thermal ignitability curve is particle size invariant for all sizes below 55 μm. It is no coincidence that essentially the same invariance is observed for the lean limit concentration measurements in a completely independent system, as indicated in figure 26. Both sets of measurements tend to confirm and corroborate one another. Essentially the same kind of behavior is observed for the flammability and ignitability domains for polyethylene (fig. 34), which is a completely volatilizable dust.

Preliminary data on the electrical spark ignition of dust clouds at ambient and above-ambient temperatures were also presented in this paper. As noted by previous researchers (21), the minimum spark ignition energy of a dust cloud decreases with increasing temperature. A more detailed study of spark ignition of dust clouds is planned for the future.

REFERENCES

1. American Society for Testing and Materials. Standard Method for Proximate Analysis of Coal and Coke. D3172-D3175 in 1981 Annual Book of ASTM Standards, Part 26: Gaseous Fuels; Coal and Coke; Atmospheric Analysis. Philadelphia, Pa., 1981, pp. 366-375.

2. Ballal, D. R., and A. H. Lefebvre. A General Model of Spark Ignition for Gaseous and Liquid Fuel-Air Mixtures. Eighteenth Symposium (International) on Combustion. The Combustion Institute, Pittsburgh, Pa., 1981, pp. 1737-1746.

3. Berg, R. H. Electronic Size Analysis of Subsieve Particles by Flowing Through a Small Liquid Resistor. ASTM, pub. 234, 1959, pp. 245-255.

4. Cashdollar, K. L., I. Liebman, and R. S. Conti. Three Bureau of Mines Optical Dust Probes. BuMines RI 8542, 1981, 26 pp.

5. Conti, R. S., K. L. Cashdollar, and I. Liebman. Improved Optical Dust Probe for Monitoring Dust Explosions. Rev. Sci. Instr., v. 53, 1982, pp. 311-313.

6. Conti, R. S., K. L. Cashdollar, I. Liebman, and M. Hertzberg. Thermal Ignition of Dust Clouds. Pres. at Fall Technical Meeting of the Eastern Section: The Combustion Institute, Pittsburgh, Pa., Oct 27-29, 1981, 4 pp.; available from Pittsburgh Research Center, Bureau of Mines, Pittsburgh, Pa.

7. Conti, R. S., M. Hertzberg, F. T. Duda, and K. L. Cashdollar. Rapid Sampling System for Dusts and Gases. Rev. Sci. Instr., v. 54, 1983, pp. 32-36.

8. Dorsett, H. G., Jr., M. Jacobson, F. J. Nagy, and R. P. Williams. Laboratory Equipment and Test Procedures for Evaluating Explosibility of Dusts. BuMines RI 5624, 1960, 21 pp.

9. Finney, C. L., and T. S. Spicer. The Ignitability of Bituminous Coal. Pennsylvania State University, University Park, Pa., Spec. Res. Rep. SR-18, 1960, 66 pp.

10. Gibson, N., and R. L. Rogers. Ignition and Combustion of Dust Clouds in Hot Environments--An Exploratory Study. Paper in Chemical Process Hazards With Specific Reference to Plant Design, Inst. of Chem. Eng. Symp. Ser. 58. Institute of Chemical Engineering, Rugby, England, 1980, pp. 209-217.

11. Godbert, A. L., and H. P. Greenwald. Laboratory Studies of the Inflammability of Coal Dust: Effect of Fineness of Coal and Inert Dusts on the Inflammability of Coal Dusts. BuMines Bull. 389, 1935, 29 pp.

12. Gray, P., J. F. Griffiths, and J. R. Bond. Carbon Monoxide Oxidation: Chemiluminescence and Ignition. Seventeenth Symposium (International) on Combustion. The Combustion Institute, Pittsburgh, Pa., 1979, pp. 811-819.

13. Hertzberg, M., K. L. Cashdollar, and C. P. Lazzara. The Limits of Flammability of Pulverized Coals and Other Dusts. Eighteenth Symposium (International) on Combustion. The Combustion Institute, Pittsburgh, Pa., 1981, p. 717-729.

14. Hertzberg, M., K. L. Cashdollar, C. P. Lazzara, and A. C. Smith. Inhibition and Extinction of Coal Dust and Methane Explosions. BuMines RI 8708, 1982, 29 pp.

15. Hertzberg, M., K. L. Cashdollar, D. L. Ng, and R. S. Conti. Domains of Flammability and Thermal Ignitability for Pulverized Coals and Other Dusts. Particle Size Dependences and Microscopic Residue Analyses. Nineteenth Symposium (International) on Combustion. The Combustion Institute, Pittsburgh, Pa., 1983, pp. 1169-1180.

16. Hertzberg, M., K. L. Cashdollar, and J. J. Opferman. The Flammability of Coal Dust-Air Mixtures. Lean Limits, Flame Temperatures, Ignition Energies, and Particle Size Effects. BuMines RI 8360, 1979, 70 pp.

17. Hertzberg, M., J. K. Richmond, and K. L. Cashdollar. Flammability Limits and the Extinguishment of Explosions in Gases, Dusts, and Their Mixtures: Theory, Experiment, and the Problem of Scale. Proc. Colloque Internat.: Berthelot-Vieille-Mallard-LeChatelier, 1st Specialists Meeting (Internat.) of the Combustion Inst,. Bordeaux, France, July 20-24, 1981. French Section of the Combustion Institute, Orleans, France, 1981, pp. 202-210.

18. Howard, J. B. Fundamentals of Coal Pyrolysis and Hydropyrolysis. Ch. 12 in Chemistry of Coal Utilization, Second Supplementary Volume, ed. by M. A. Elliott. Wiley-Interscience, New York, 1981, pp. 665-784.

19. Humphrey, H. B. Historical Summary of Coal-Mine Explosions in the United States, 1810-1958. BuMines Bull. 586, 1960, 280 pp.

20. Kuchta, J. M., A. Bartkowiak, and M. G. Zabetakis. Autoignition of Hydrocarbon Jet Fuel. BuMines RI 6654, 1965, 25 pp.

21. Lee, R. S., D. F. Aldis, D. W. Garrett, and F. S. Lai. Improved Diagnostics for Determination of Minimum Explosive Concentration, Ignition Energy and Ignition Temperature of Dusts. Powder Technol., v. 31, 1982, pp. 51-62.

22. Lewis, B., and G. von Elbe. Combustion Flames and Explosions of Gases. Academic Press, New York, 2d ed., 1961, pp. 22-64.

23. Liebman, I., and J. K. Richmond. Ranking of Extingushing Agents Against Coal Dust Explosions. Proc. 18th Int. Conf. of Scientific Research in the Field of Safety at Work in Mining Industry, Dubrovnik, Yugoslavia, Oct. 7-14, 1979, paper B-6, p. 329; available for consultation at the Pittsburgh Research Center, Bureau of Mines, Pittsburgh, Pa.

24. Litchfield, E. L. Minimum Ignition-Energy Concept and Its Application to Safety Engineering. BuMines RI 5671, 1959, 10 pp.

25. Nagy, J., H. G. Dorsett, Jr., and A. R. Cooper. Explosibility of Carbonaceous Dusts. BuMines RI 6597, 1965, 30 pp.

26. Nagy, J., and J. Surincik. Thermal Phenomena During Ignition of a Heated Dust Dispersion. BuMines RI 6811, 1966, 25 pp.

27. National Fire Protection Association (Boston, Mass.). Fire Protection Handbook. 14th ed., 1976, pp. 3-106 - 3-118.

28. Ng, D. L., K. L. Cashdollar, M. Hertzberg, and C. P. Lazzara. Electron Microscopy Studies of Explosion and Fire Residues. BuMines IC 8936, 1983, 63 pp.

29. Richmond, J. K., G. C. Price, M. J. Sapko, and E. M. Kawenski. Historical Summary of Coal Mine Explosions in the United States. 1959-81. BuMines IC 8909, 1983, 53 pp.

30. Richmond, J. K., M. J. Sapko, and L. F. Miller. Fire and Explosion Properties of Oil Shale. BuMines RI 8726, 1982, 39 pp.

31. Stanfield, K. E., and I. C. Frost. Method of Assaying Oil Shale by a Modified Fischer Retort. BuMines RI 4477, 1949, 13 pp.

32. Zabetakis, M. G. Flammability Characteristics of Combustion Gases and Vapors. BuMines Bull. 627, 1965, 121 pp.

33. Zabetakis, M. G., A. L. Furno, and G. W. Jones. Minimum Spontaneous Ignition Temperatures of Combustibles in Air. Ind. and Eng. Chem., v. 46, 1954, pp. 2173-2178.

☆U.S. GOVERNMENT PRINTING OFFICE: 1983-605-015/66

INT.-BU.OF MINES,PGH.,PA. 27048